PEOPLE'S DEMOCRATIC REPUBLIC OF ALGERIA
MINISTRY OF HIGHER EDUCATION AND SCIENTIFIC RESEARCH
University Amar Telidji- Laghouat

DOMAIN: Sciences and Technology

FIELD: Electrical Engineering

OPTION: Electrical Power System

FACULTY: Technology

DEPARTMENT: Electrotechnic

MASTER MEMOIR

Presented by: BENLAHBIB Nafissa

MAICHA Rayhane

Theme

Load Frequency Control Strategy for Wind Power Connected Power System

Defense jury:

Full Name	**Grade**	**Quality**
CHETTIH Saliha	Prof	President
ARIF Salem	Prof	Examiner
OUBBATI Youcef	M.C.B	Supervisor
HALMOUS Abdelkader	PhD Student	Co-Supervisor

Academic Year: 2021-2022

الملخص

تتناول هذه المذكرة مشكلة أنظمة المراقبة الثانوية في نظام حراري ذو ثلاث مناطق مترابطة فيما بينها و اخذنا بعين الاعتبار القيود (GDB) و (GRC) من اجل دراسة اكثر واقعية،و لأجل هذا استخدمنا وحدات التحكمPID تم تحديد اعدادات PIDالمثلى من خلال خوارزمية تحسين جديدة تسمى Archimedes optimization algorithm (AOA) و النظام الخوارزمي الوراثي (GA)و تمت المقارنة بينهما.بعد ذلك نظهر تأثير دمج طاقة الرياح في المنطقة الأولى للنظام ثم تم اقتراح نظام تخزين طاقة البطاريات BESSفي كل مناطق النظام لإسترجاع تردد النظام ضد مختلف الاضطرابات الناتجة عن دمج طاقة الرياح

الكلمات المفتاحية: التحكم في تردد الحمل، أنظمة الطاقة الحرارية المترابطة، طاقة الرياح خوارزمية ارخميدس للتحسين ،الخوارزمية الوراثية ،نظام تخزين طاقة البطاريات

Abstract

This dissertation treats problem of Load Frequency Control (LFC) with the integration of Renewable Energy sources (Res) in a three-area interconnected thermal power system taking into consideration Generation Rate Constraint (GRC) and Speed Governor Dead-Band (GDB) for a more realistic study. For this purpose, we used PID controllers in our system. The optimum PID settings were determined by two optimization methods, a new algorithm called Archimedes Optimization Algorithm (AOA) and Genetic Algorithm (GA), and compared to each other. After that, we show the impact of the integration of Wind power in one area in our system. Then, we propose the Battery Energy Storage System (BESS) in all areas to restore system frequency against various disruptions produced by wind power integration.

Key words: Load Frequency Control, Interconnected Thermal Power System, Wind Power, Archimedes Optimization Algorithm (AOA), Genetic Algorithm (GA), Battery Energy Storage system (BESS).

Résumé

Cette mémoire traite le problème du contrôle de la fréquence de la charge (LFC) avec l'intégration des sources d'Énergie Renouvelables (REs) dans un système électrique thermique interconnecté à trois zones en prenant en considération la contrainte du taux de génération (GRC) et la bande morte du régulateur de vitesse (GDB) pour une étude plus réaliste. À cette fin, nous avons utilisé des contrôleurs PID dans notre système. Les paramètres PID optimaux ont été déterminés par deux méthodes d'optimisation, un nouvel algorithme appelé Algorithme d'Optimisation d'Archimède (AOA) et l'Algorithme Génétique (GA), et comparés entre eux. Ensuite, nous montrons l'impact de l'intégration de l'énergie éolienne dans une zone de notre système. Puis, nous proposons le système de stockage d'énergie par batterie (BESS) dans toutes les zones pour restaurer la fréquence du système contre les diverses perturbations produites par l'intégration de l'énergie éolienne.

Mots clés : Contrôle de la Fréquence de Charge, Système de Puissance Thermique interconnecté, Énergie éolienne, Algorithme d'Optimisation d'Archimède, Algorithme Génétique, Système de Stockage d'Energie par Batterie

Dedication

I would like to dedicate this work
To my parents who always picked me up on time and encouraged
me;
To grandmothers and grandfathers;
To my brother and sisters;
To all my family;
To my dear friend HANANE;
To everyone who taught me a character,
shining the way in front of me.

Nafissa

Dedication

I dedicate this work to the memory of my grandfather's

To my grandmother,

To my parents,

To my brothers and sisters,

To all my family members,

To my dear friends

RAYHANE

Acknowledgement

We would like to express our deepest gratitude to our supervisors **Dr. OUBBATI Youcef** and **Dr. HALMOUS Abdelkader** for their immeasurable supports, good guidance and constructive criticism given to us throughout the preparation of this work.

In particular, their gentle and compassionate approach of supervision crucially helped to render the thesis journey a pleasant experience. Without them, this research would not have been possible and we thank also the members of the jury **Pr. ARIF Salem** and **Pr. CHETTIH Saliha** for reading and evaluating our thesis.

We would like to extend our sincere thanks to teachers and professors who have given us their knowledge and helped us along the way.

Acknowledgement ..... **I**
List of Figures ..... **IV**
List of Tables ..... **V**
Nomenclature ..... **VI**
General Introduction ..... **I**
Problematic 1
A brief survey of the LFC literature 1
Objectives of this dissertation 2
Dissertation outlines 2
1 Chapter 1: Frequency Regulation in Power System **5**
1.1 Introduction 5
1.2 Frequency regulation in power system 5
1.3 Automatic Generation Control 7
1.4 Power generating units 8
1.4.1 Turbines 8
1.4.2 Generators 9
1.4.3 Governors 11
1.5 Proportional Integral Derivative Regulator 12
1.6 AGC in multi-area system 13
1.6.1 Two area system with primary control 13
1.6.2 Two area system with secondary control 15
1.7 The interconnected power systems 16
1.7.1 Tie-lines 16
1.7.2 Area Control Error 17
1.8 Physical constraints 18
1.8.1 Generation rate constraint (GRC) 18
1.8.2 Governor Dead Band (GDB) 19
1.9 Conclusion 20
2 Chapter 2:Wind Power, BESS and Optimization **22**
2.1 Introduction 22
2.2 What is Renewable Energy? 22
2.2.1 Renewable energy resources 22
2.2.2 Integration of renewable energy sources: 23

2.3 Optimization 26
2.3.1 Classification 27
2.3.2 Archimedes' optimization algorithm (AOA) 28
2.3.3 Optimization of Regulator Parameters 35
2.4 Battery Energy Storage System (BESS) 36
2.4.1 Benefits of BESS 36
2.4.2 Modelling of BESS 36
2.5 Conclusion: 37
3 Chapter 3: Simulation and Results 39
3.1 Introduction 39
3.2 The problem's Formulation 39
3.3 Investigated power system 40
3.4 Cases Study 41
3.4.1 Case-1 41
3.4.2 Case-2 44
3.4.3 Case-3 45
3.4.4 Case-4 53
3.5 Conclusion 57
General conclusion 59
References 62
Appendix 66
Appendix A 67
Appendix B 68

List of Figures

1.1: Balance generation load 6

1.2: Block diagram scheme of asynchronous generation based on primary and secondary frequency control loops 6

1.3: Synchronous Generators LFC, and AVR schematic diagram 7

1.4: Block diagram of the generator 10

1.5: Block diagram of the generator with Load damping effect 10

1.6: Reduced block diagram of the generator with Load damping effect 11

1.7: Schematic diagram of speed governing unit 12

1.8: Reduced block diagram of the speed governing unit 12

1.9: PID control scheme “parallel form” 13

1.10: Equivalent network for two area power system 14

1.11: Two interconnected area system with only primary LFC loop 15

1.12: Two interconnected area system with secondary control loop 16

1.13: Block diagram of tie-lines 17

1.14: GRC models (a) Closed Loop modeling, (b) Open Loop modeling 19

1.15: Block diagram model of speed governor dead-band 19

2.1: Renewable energy sources 23

2.2: Rotor area and hub height of wind turbines since 1980 25

2.3: Local and Global Optimal Solution 26

2.4: Classification of optimization methods 28

2.5: (a) An Object is immersed in a fluid, and (b) the volume of fluid displaced 29

2.6: Many objects immersed in the same fluid 30

2.7: Different Existing performance Criteria 35

2.8: BESS First Order Transfer Function model 36

3.1: Three areas LFC test system with integration of wind power 41

3.2: Three areas LFC test System with 1% Load variation in area 1 42

3.3: Frequency dynamical response of the first area for the different constraints 42

3.4: Comparison between AOA and GA using ISE criterion 44

3.5: Three areas LFC system With Power Wind 44

3.6: Dynamical response of frequency deviation area 1 with Wind Power 45

3.7: Three areas LFC System with BESS.....46
3.8: Comparison of system without BESS, with BESS of ISE value.....46
3.9: Dynamic response of (a): Δf_1, (b): Δf_2 and (c): Δf_3 with and without BESS.....48
3.10: Dynamic response of (a): ACE_1, (b): ACE_2 and (c): ACE_3 with and without BESS.....49
3.11: Dynamic response of (a): ΔP_{m1}, (b): ΔP_{m2} and (c): ΔP_{m3}.....51
3.12: Dynamic response of (a): ΔP_{tie13}, (b): ΔP_{tie12} and (c): ΔP_{tie23}.....52
3.13: Three areas LFC test system with wind power and BESS.....53
3.14: Dynamical response of (a): $\Delta f1$, (b): $\Delta f2$ and (c): $\Delta f3$ with integration of wind power and BESS.....55
3.15: Dynamic response of (a): ΔP_{tie13}, (b): ΔP_{tie12} and (c): ΔP_{tie23} with integration of wind power and BESS.....56
3.16: Comparison of ISE value of integration of Wind power ana BESS.....57

List of Tables

2.1: Pseudo code of AOA.....34
2.2: Battery charging status based on system Frequency.....37
3.1: Parameter Settings of GA and AOA.....40
3.2: Optimal controller's settings using ISE criterion (GA).....43
3.3: Optimal controller's settings using ISE criterion (AOA).....43
3.4: Settling Time and Peak Overshoot/Undershoot for Case-3.....53

Nomenclature

Symbols:

A	Wind turbine's rotor area
a	The gravity or acceleration
B	Fluid
C_p	Aerodynamic efficiency
D	Load damping constant
F_b	Buoyant force
f	Frequency (Hz).
f_{ref}	Rated frequency
F_{hp}	High-pressure stage rating
K_p	Gain of the proportional action
K_i	Gain of the integral action
K_d	Gain of the derivative action
M_s	Inertia constant of the generator
o	Immersed object
R_T	Temporary droop
R	Permanent droop
R	Speed regulation characteristic
T_{ch}	Time delay
T_D	Derivative time constant.
T_g	Time constant of the governor

T_I	Integral time constant
T_R	Reset time
T_{rh}	Low pressure reheat time
T_w	Water starting time
V	Wind speed
v	The volume
W_o	Object's weight
X_{tie}	Tie line reactance
Δf	Frequency deviation (Hz)
ΔP_m	Mechanical Power deviation (pu)
ΔP_C	Power deviation (pu)
ΔP_L	Load variation (pu)
ΔP_{Tie}	Tie line power deviation (pu)
ΔP	Valve position change (pu)
ΔP_{el}	Electrical powers
$\Delta \omega r$	Rotor speed deviation
ρ	Density
θ	Pitch angle
λ	Tip speed ratio

Acronyms and abbreviations

ACE Area Control Error

AGC Automatic Generation Control

AOA Archimedes' optimization algorithm

AVR Automatic Voltage Regulator

BESS Battery Energy Storage System

FCLs Frequency Control Loops

GA Genetic Algorithm

GDB Governor Dead-Band

GRC Generation Rate Constraint

ISE Integral of the Squared Error

PID Proportional Integral Derivative

PO Peak Overshoot

PU Peak Undershoot

RE Renewable Energy

RESs Renewable Energy Sources

ST Settling Time

WT Wind Turbine

General Introduction

Problematic

The fundamental goal of a power system is to generate and transport electrical power as inexpensively and efficiently as possible with renewable energy sources (wind power) while controlling the frequency within acceptable bounds. So, the operator must ensure a permanent equilibrium between the total generated power with the total load demand. The kinetic energy from wind energy is converted into mechanical energy. This mechanical energy is then transferred to the rotor of the generator. The wind turbine consists of a turbine-generator shaft mechanism, which is used to convert the rotor rotation into electrical energy, which will result in disturbances in the balance [1,2].

For this reason, we have introduced the Load Frequency Control (LFC), whose role is:

- To regulate the frequency to its specified nominal value;
- To maintain the interchange power between control areas at the scheduled values;
- To distribute the required change in generation among units to minimize the operating costs.

Generally, there are four control loops in the AGC problem. We can site the well-treated ones:

- Primary Control Loop (PCL)

The function of PCL is to re-establish a balance between generation and load at a frequency different from its nominal value.

- Secondary Control Loop (SCL)

The function of SCL, called Load Frequency Control (LFC), is to restore cross-border power exchanges to their set-point values and the System Frequency to its set-point value simultaneously.

A brief survey of the LFC literature

The LFC problem in power systems has a long history. In a power system, LFC as an ancillary service acquires an essential and fundamental role in maintaining the electrical system reliability at an adequate level [3].

The LFC scheme has evolved over the past few decades and is used on interconnected power systems. There has been continuing interest in designing LFC with better performance to maintain the frequency and keep tie-line power flows within prespecified values using various control strategies [3].

For a more realistic study, several non-linear constraints such as Governor Dead Band (GDB), Generation Rate constraint (GRC), Dynamic Boiler (DB), and Time Delay (TD) have been introduced [4,5].

Objectives of this dissertation

The main objectives of this memoir are presented as follows:

- To review the effect of different constraints such as GDB and GRC in the system performance;
- To optimize the parameter of PID controller using different methods of genetic optimization algorithm (GA), Archimedes Optimization algorithm (AOA)
- To plant the renewable energy in an interconnected power system;
- To show the impact of wind power on our system;
- To verify the role of the Battery Energy Storage System;

Dissertation outlines

The three main chapters of this dissertation are as follows

Chapter 1

- This chapter will present some basic information about Load Frequency Control (LFC) problems in interconnected power systems. Then, different models are described, and the controller PID is presented. Finally, nonlinear constraints such as GRC and GDB are introduced into the system for a more realistic investigation.

Chapter 2

- In this chapter, we will present the impact of wind power on the power system. Then, we highlighted the optimization of Regulator Parameters and showed the different performance criteria used for the controller synthesis. Following that, the generality of

met-heuristics and a new optimization algorithm are discussed. Finally, we explore battery energy storage systems and their benefits.

Chapter 3

- The investigation is performed on a three-area reheat-thermal system, considering GRC and GDB for a more realistic study with the integration of wind power. Then, the optimal controller setting is determined via a new optimization algorithm known as AOA by Integral of Square Error (ISE). After that, the AOA algorithm is compared with the Genetic algorithm (GA) to ensure that it is effective. Then, it shows the impact of wind power on the power system. Finally, we compared the performance of the system with and without BESS by considering integration wind power into our system.

Finally, we end our memoir with the main conclusions and some prospects for future research.

Chapter 1: Frequency Regulation in Power System

1.1 Introduction

Load frequency control (LFC) is an essential issue in power system operation and control for supplying sufficient and reliable electric power with good quality. In this chapter, Automatic generation control will be briefly discussed. Next, the power system's load frequency control concept will be introduced. Moreover, finally, several non-linear constraints will be outlined.

1.2 Frequency regulation in power system

Severe system stress resulting in an imbalance between load and generation seriously degrades the power system performance and even stability. This usually slow phenomenon must be considered in the power system frequency control problem.

Frequency deviation directly results from an imbalance between the electrical load and the power supplied by the connected generators.

Hence, it offers a helpful index to designate the generation and load imbalance, as exposed in Figure 1.1. Different Frequency Control Loops (FCLs) may be required to maintain power system frequency stability depending on the frequency deviation range.

Figure 1.2 illustrates the conventional FCLs [6].

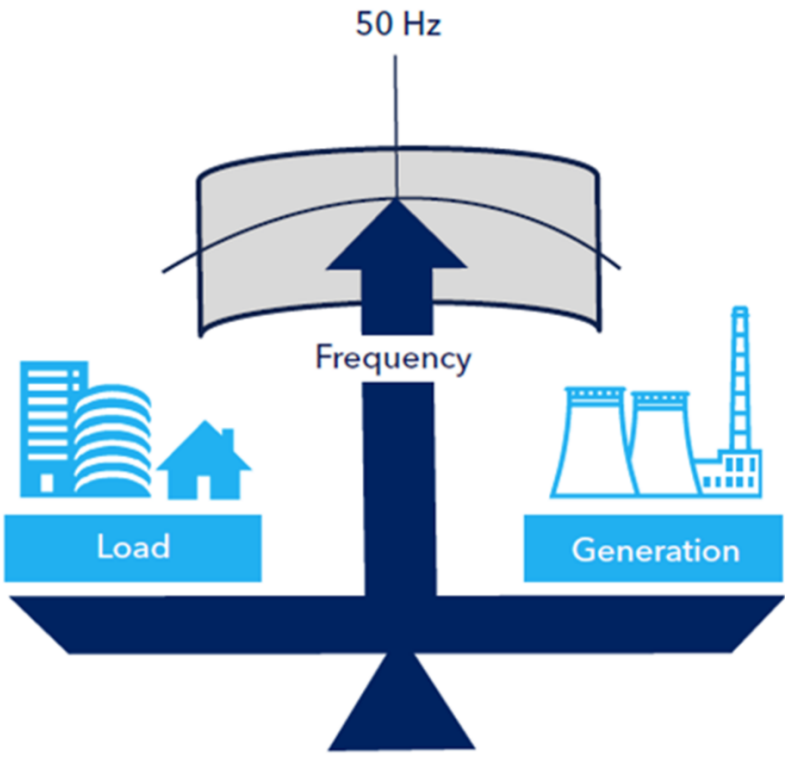

Figure 1.1: Balance generation load

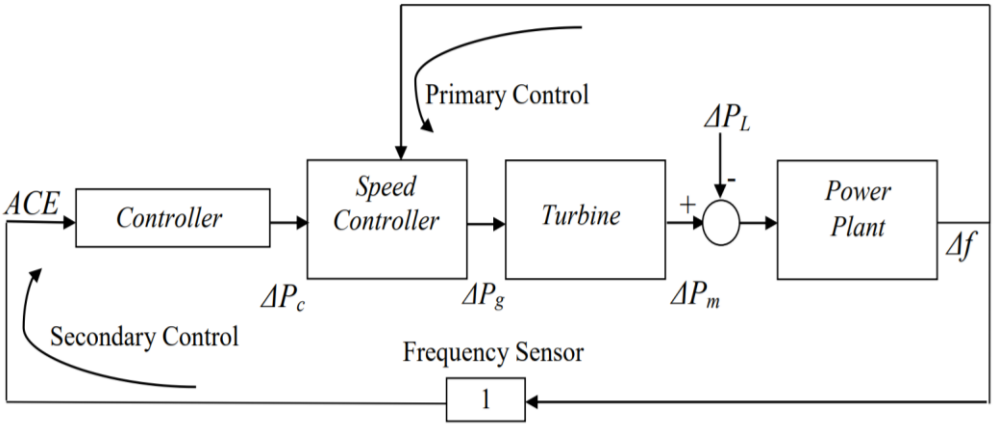

Figure 1.2: Block diagram scheme of asynchronous generation based on primary and secondary frequency control loops

1.3 Automatic Generation Control

To preserve voltage and frequency in a rated value, AGC is installed on each generator. The primary responsibility of an AGC is to ensure that an electric power system runs smoothly and efficiently. AGC aims to enable each generator to control its generation independently to achieve zero steady-state value of area control error and economic loadings of its generators against random variations in the load demand, which occur continuously in a power system. As a result, to ensure an adequate power supply, an AGC system must complement current and sophisticated control approaches. So, AGC has become an important issue in power system control and operation. The turbine speed reduces when the load on the power system increases before the governor readjusts the steam/water input to the new load. The error signal gets smaller as the variation in the value of speed decreases, and the orientations of the governor fly-balls get closer to the point required to preserve a constant speed [6-8].

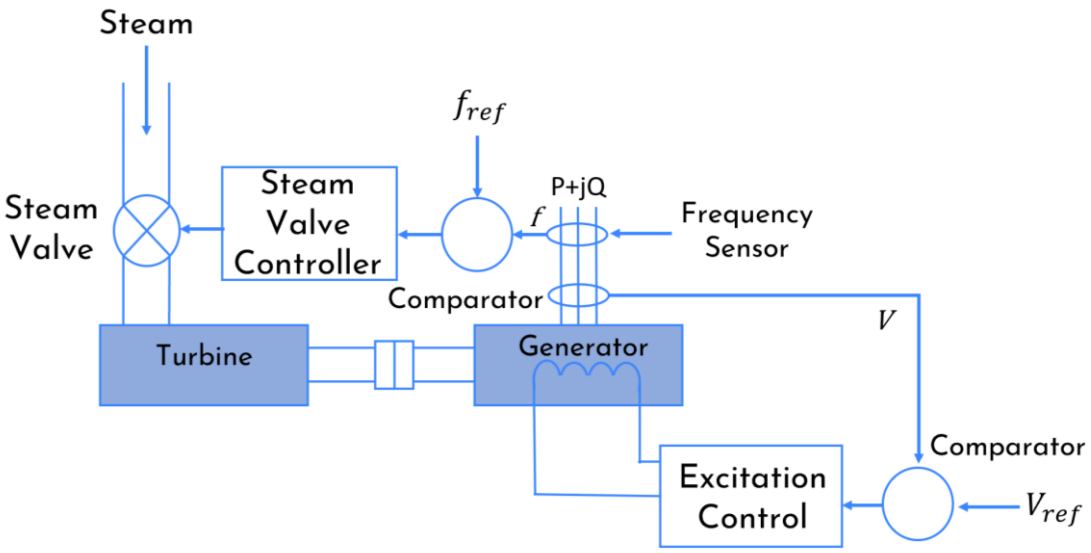

Figure1.3: Synchronous Generators LFC, and AVR schematic diagram

The schematic diagram comprises two control mechanisms. The first is frequency control, and the second is voltage control. The frequency sensor senses the frequency and provides it to a frequency comparator for the first case. Then the comparator compares the actual frequency with the rated frequency (f_{ref}) and generates an error signal. This signal is then provided to steam valve control (thermal) or governor (hydro). Then the steam valve/governor regulates the opening and closing of the steam valve/wicket gate. Then the

regulated gate is provided to the turbine, which is coupled to a generator. For the second case, voltage sensors sense the voltage and provide it to the comparator. Thus, the comparator compares the actual voltage value with the reference voltage (V_{ref}) and generates the error signals. The signal is provided to excitation control, and accordingly, the excitation control is coupled with the generator. Hence, the frequency and voltage sensor sense the frequency and voltage output. Controllers, on the other hand, are designed for a particular set of operating parameters, and they handle small fluctuations in load demand without frequency, as well as voltage beyond the permitted limits [9].

Power systems frequency can be controlled using dual control loops, namely primary and secondary loops. The primary control loop prevents instant variations in the frequency before triggering the frequency protection switches. It is provided through the governor droops that typically give rise to the steady-state error. Secondary control is an Automatic Load frequency Control (ALFC) implemented to control the system frequency to its expected value in the power system network [10].

1.4 Power generating units

1.4.1 Turbines

A turbine unit in power systems transforms the natural energy, such as the energy from steam or water, into mechanical power (ΔP_m) that is supplied to the generator. There are three kinds of commonly used turbines in the LFC model: non-reheat, reheat, and hydraulic turbines, all of which can be modeled by transfer functions.

Non-reheat turbines are first-order units. A time delay (denoted by Tch) occurs between switching the valve and producing the turbine torque. The transfer function can be of the non-reheat turbine is represented as:

$$G_{NR}(s) = \frac{\Delta p_m(s)}{\Delta p_v(s)} = \frac{1}{T_{ch}S+1} \tag{1.1}$$

where ΔP_V is the valve/gate position change [11].

Reheat turbines are modeled as second-order units since they have different stages due to high and low steam pressure. The transfer function can be represented as:

$$G_R(s) = \frac{\Delta p_m(s)}{\Delta p_v(s)} = \frac{F_{hp}T_{rh}s+1}{(Tch\ S+1)(T_{rh}s+1)} \quad (1.2)$$

where T_{rh} stands for the low pressure reheat time and F_{hp} represents the high-pressure stage rating [12].

Hydraulic turbines are non-minimum phase units due to water inertia. In the hydraulic turbine, the water pressure response is opposite to the gate position change at first and recovers after the transient response. Thus, the transfer function of the hydraulic turbine is in the form of:

$$G_H(s) = \frac{\Delta p_m(s)}{\Delta p_v(s)} = \frac{-T\omega S+1}{(T\omega/2)S+1} \quad (1.3)$$

where T_ω is the water starting time [11].

For stability concerns, a transient droop compensation part in the governor is needed for the hydraulic turbine. The transfer function of the transient droop compensation part is given by:

$$G_{TDC}(s)\frac{T_R S+1}{T_R(R_T/R)S+1} \quad (1.4)$$

where T_R, R_T and R represent the reset time, temporary droop and permanent droop respectively [11].

1.4.2 Generators

A generator unit in power systems converts the mechanical power received from the turbine into electrical power. However, for LFC, we focus on the generator's rotor speed output (frequency of the power systems) instead of the energy transformation. Since electrical power is hard to store in large amounts, the balance between the generated power and the load demand has to be maintained.

Once a load change occurs, the mechanical power sent from the turbine will no longer match the electrical power generated by the generator. This error between the mechanical (ΔP_m) and electrical powers (ΔP_{el}) is integrated into the rotor speed deviation ($\Delta\omega r$), which can be turned into the frequency bias (Δf) by multiplying by 2π. The relationship between ΔP_m and Δf is shown in Figure 1.4, where M is the inertia constant of the generator [11].

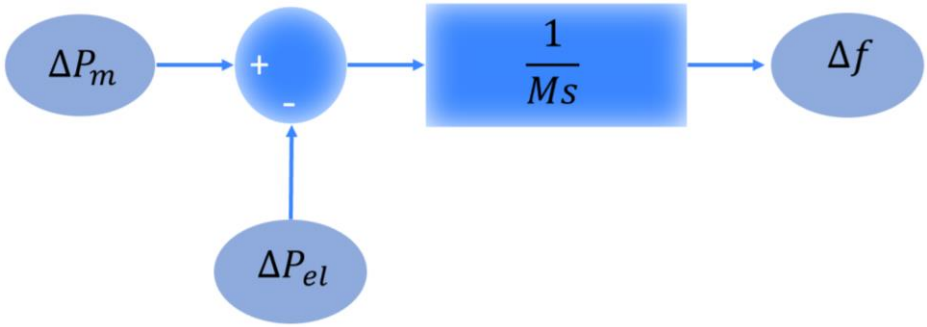

Figure1.4: Block diagram of the generator

The power loads can be decomposed into resistive loads (ΔP_L), which remain constant when the rotor speed changes, and motor loads that change with load speed. If the mechanical power remains unchanged, the motor loads will compensate for the load change at a rotor speed different from a scheduled value, shown in Figure 1.5, where D is the load damping constant [11].

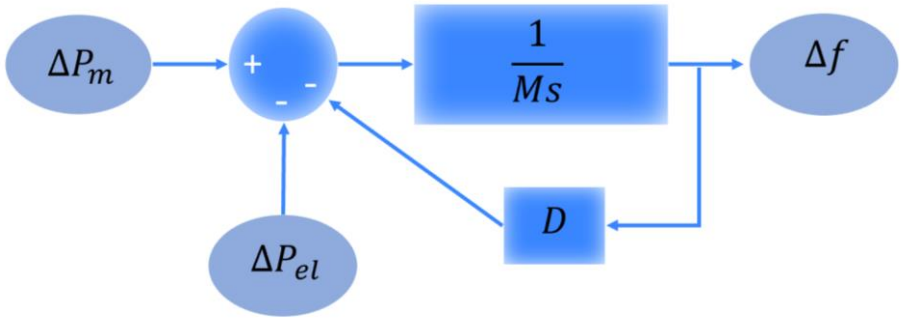

Figure1.5: Block diagram of the generator with load damping effect

The reduced form of Figure 1.5 is shown in Figure 1.6, which is the generator model that we plan to use for the LFC design. The Laplace-transform representation of the block diagram in Figure 1.6 is:

$$\Delta P_m(s) - \Delta P_L(s) = (Ms + D)\Delta f(s) \quad (1.5)$$

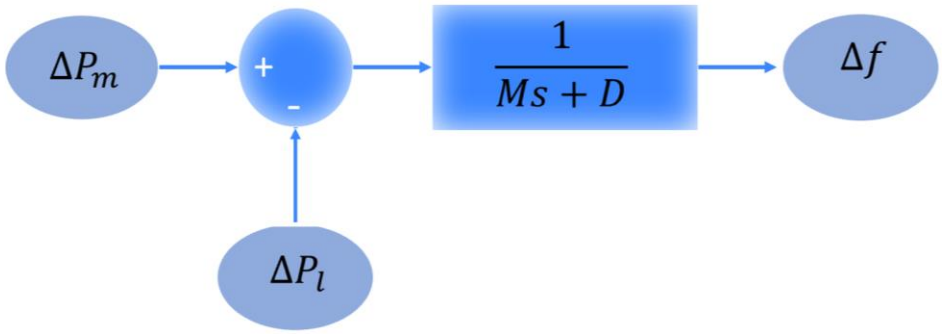

Figure1.6: Reduced block diagram of the generator with Load damping effect.

1.4.3 Governors

Governors are the units used in power systems to sense the frequency bias caused by the load change and cancel it by varying the inputs of the turbines. The schematic diagram of a speed governing unit is shown in Figure 1.7, where R is the speed regulation characteristic, and T_g is the time constant of the governor. If without load reference, when the load change occurs, part of the change will be compensated by the valve/gate adjustment, while the rest is represented in the form of frequency deviation. The goal of LFC is to regulate frequency deviation in varying active power loads. Thus, the load reference setpoint can adjust the valve/gate positions so that the power generation cancels all the load change rather than resulting in a frequency deviation [11].

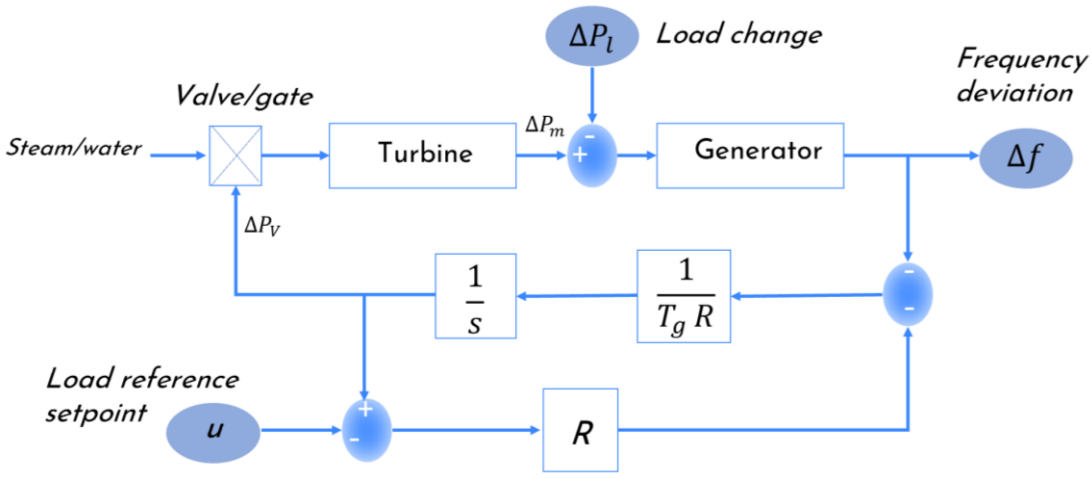

Figure1.7: Schematic diagram of speed governing unit

The reduced form of Figure 1.7 is shown in Figure 1.8 The Laplace transform representation of the block diagram in Figure 1.8 is given by:

$$u(s) - \frac{\Delta f(s)}{R} = (T_g S + 1)\Delta P_v(s) \tag{1.6}$$

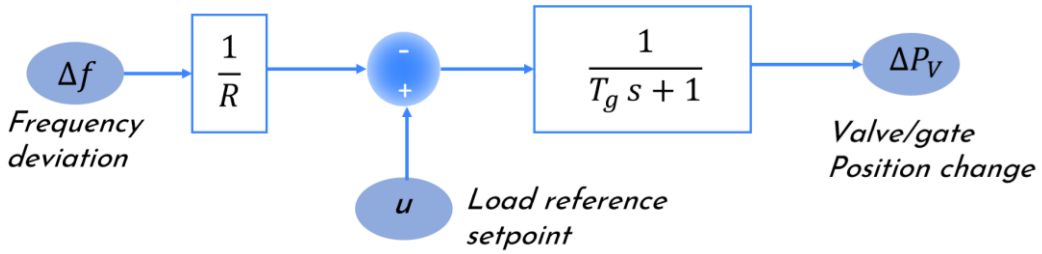

Figure1.8: Reduced block diagram of the speed governing unit

1.5 Proportional Integral Derivative Regulator

A PID controller may be considered an extreme form of a phase lead-lag compensator with one pole at the origin and the other at infinity. Similarly, the PI and the PD controllers can also be regarded as extreme forms of phase-lag and phase-lead compensators, respectively. A standard PID controller is also known as the “three-term” controller, whose transfer function is generally written in the “parallel form” given by (1.7) or the “ideal form” given by (1.8):

$$G(s) = K_P + K_I \frac{1}{s} + K_D S \tag{1.7}$$

$$G(s) = K_P \left(1 + \frac{1}{T_I S} + T_D S\right) \tag{1.8}$$

Where K_P is the proportional gain, K_I is the integral gain, K_D is the derivative gain, $T_I$is the integral time constant and, T_D is the derivative time constant. The "three-term" functionalities are highlighted by the following [13].

- The proportional term: providing an overall control behavior equals the error signal through the all-pass gain factor.
- The integral term: reducing steady-state errors through low-frequency compensation by an integrator.
- The derivative term: improving transient response through high-frequency compensation by a differentiator.

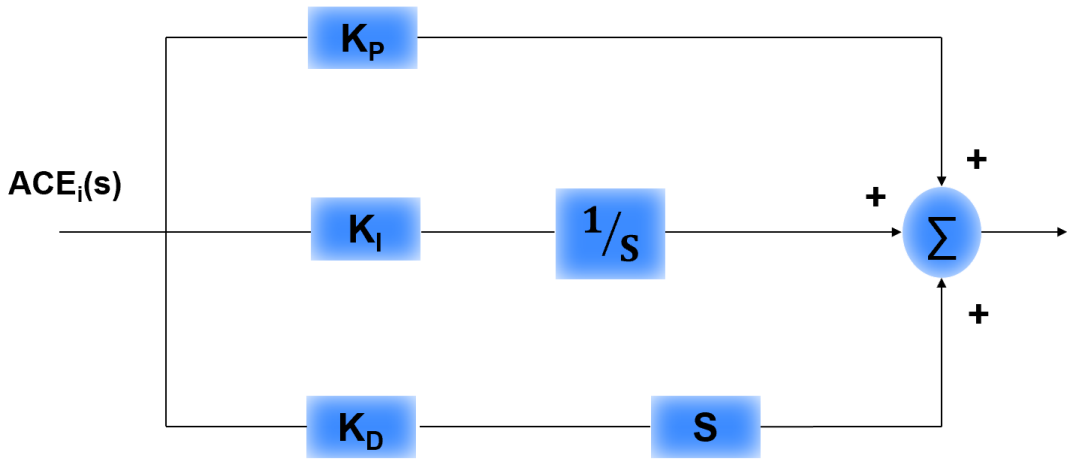

Figure1.9: PID control scheme "parallel form"

1.6 AGC in multi-area system

1.6.1 Two area system with primary control

Consider two areas represented by an equivalent generating unit interconnected by a lossless tie line with X_{tie}reactance. Each region is represented behind an equivalent reactance by a voltage source, as shown in Fig. 1.10 [11].

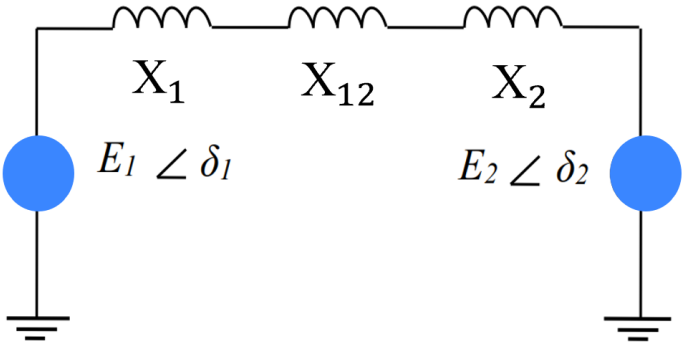

Figure1.10: Equivalent network for two area power system

The real power transferred over the tie line is given during normal operation by:

$$P_{12} = \frac{|E_1||E_2|}{X_{12}} \sin \delta_1 \tag{1.9}$$

Where: $X_{12} = X_1 + X_{tie} + X_2$, and $\delta_{12} = \delta_1 - \delta_2$

The tie line power deviation then takes on the form:

$$\Delta P12 = P2(\Delta\delta 1 - \Delta\delta 2) \tag{1.10}$$

The tie line power flow appears to increase the load in one area and decrease the load in the other, depending on the direction of the flow. The direction of the current is dictated by the difference in the angle of phase; if $\Delta\delta_1 > \Delta\delta_2$, the power flows from area 1 to area 2 [14].

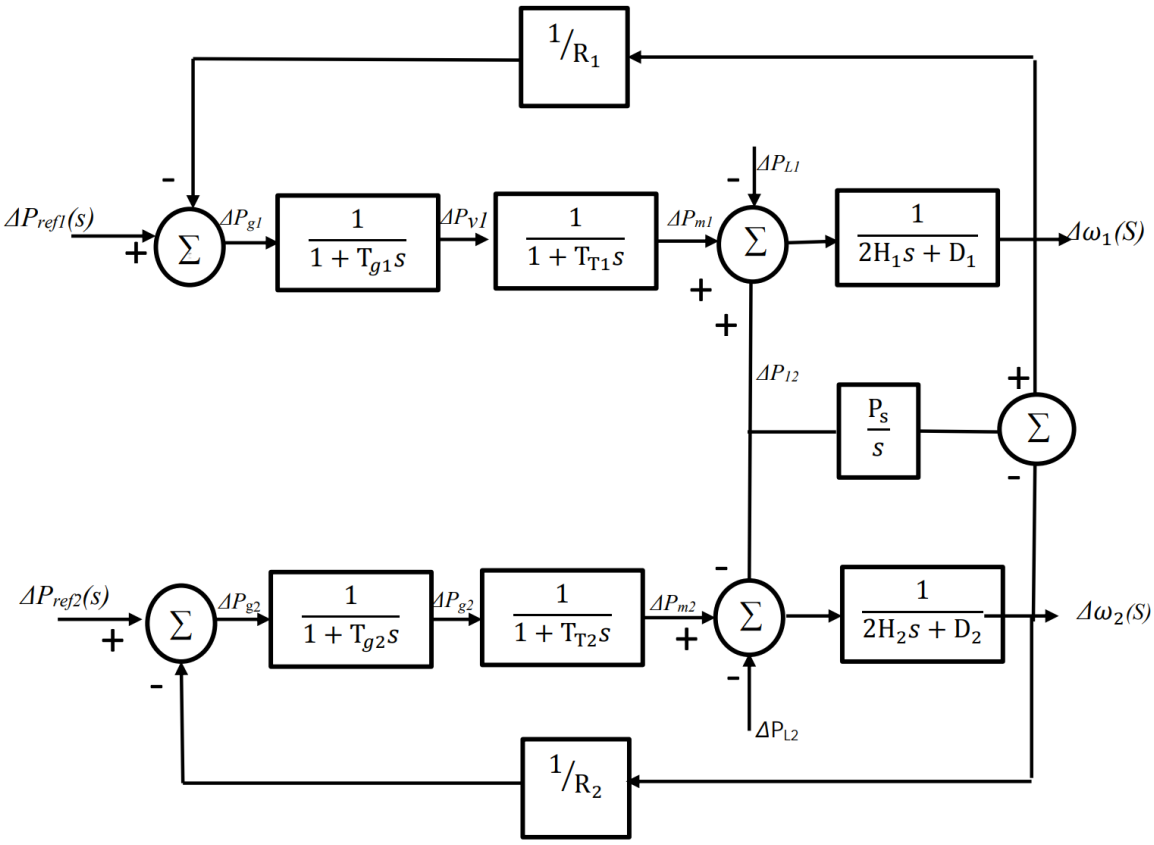

Figure1.11: Two interconnected area system with only primary LFC loop

1.6.2 Two area system with secondary control

The power system works in the normal operating state so that the demands of the areas are met at nominal frequency for normal mode, a simple control strategy is [15]:

- To keep the frequency at a nominal value;
- To maintain the tie-line flow at about schedule;
- Each area will absorb its own load charges.

Conventional LFC is based on tie-line bias management, where each area tends to reduce ACE to zero; for each region, the control error appears to consist of a linear combination of frequency and tie-line error:

$$ACE_i = \sum_{j=1}^{n} \Delta P_{ij} + K_i \Delta\omega \qquad (1.11)$$

The area bias Ki determines how much interaction there is in neighboring areas during a disturbance. An overall satisfying result is obtained when K is selected equal to the frequency bias factor of that area, i.e., Bi = 1/Ri + Di. Thus, the ACEs for two area systems are:

$$\mathrm{ACE1} = \Delta P12 + \mathrm{B1}\Delta\omega 1 \tag{1.12}$$

$$\mathrm{ACE2} = \Delta P21 + \mathrm{B2}\Delta\omega 2 \tag{1.13}$$

Wherever ΔP_{12} and ΔP_{21} are departures from scheduled interchanges, ACEs are used as actuating signals to cause changes in reference power setting points, and when steady state is reached, ΔP_{12} and $\Delta\omega$ will be zero. The integrator gain constant must be chosen low enough to not trigger the area to enter a mode of chase. Figure 1.12 displays the block diagram of a basic AGC for two area system [14].

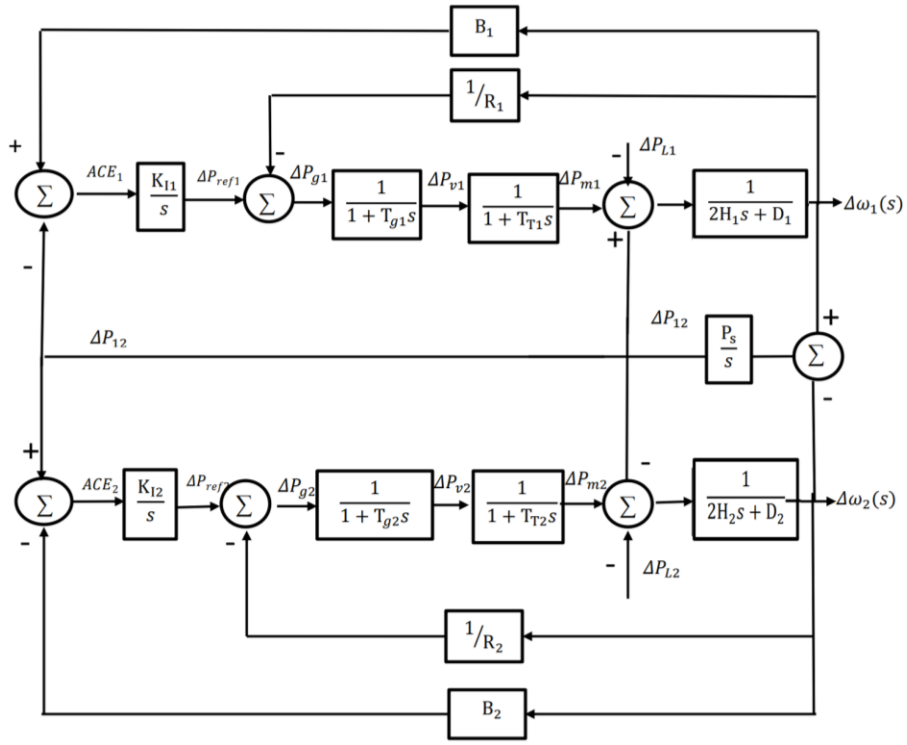

Figure1.12: Two interconnected area system with secondary control loop

1.7 The interconnected power systems

1.7.1 Tie-lines

In an interconnected power system, different areas are connected via tie-lines. When the frequencies in the two areas are different, a power exchange occurs through the tie-line

that connects the two areas. The tie-line connections can be modeled as shown in Figure 1.13. The Laplace transform representation of the block diagram in Figure 1.13 is given by:

$$\Delta P_{\text{tie } ij}(s) = \frac{1}{s} T_{ij}\left(\Delta f_i(s) - \Delta f_j(s)\right) \quad (1.14)$$

where $\Delta P_{\text{tie ij}}$ is tie-line exchange power between areas i and j, and T_{ij} is the tie-line synchronizing torque coefficient between area i and j [11]. From Figure 1.13, we can see that the tie-line power error is the integral of the frequency difference between the two areas

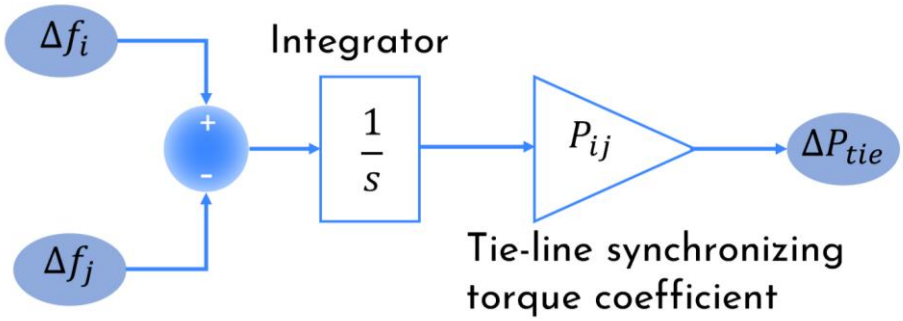

Figure1.13: Block diagram of tie-lines

1.7.2 Area Control Error

The conventional LFC is composed of a frequency sensor and an integrator. The frequency sensor measures the frequency error Δf and feeds this error signal into the integrator. The input to the integrator is called the Area Control Error (ACE). The ACE is defined as the change in area frequency, which forces the steady-state frequency error to zero, when used in an integral-control loop[16]. The control error for each area consists of a linear combination of frequency and tie-line error. Area Control Error is defined by:

$$ACE_i = \sum_{j=1}^{n} \Delta P_{ij} + K_i \Delta\omega \quad (1.15)$$

Were:

i= control area for which ACE is being measured

ΔP_{ij}= power interchange in areas i and j

K_i= control area frequency bias coefficient

$\Delta\omega$ = deviation in frequency

ACE is an error signal consisting of two terms. The first term represents the tie-line error in the scheduled power flows. The second term is inter-area assistance in generation from the control area to prevent significant deviation of interconnection frequency. ACE represents the generation versus load mismatch for the control area and indicates when total generation must be raised or lowered. Ideally, the ACE signal should be kept from becoming too large and should not be allowed to 'drift'[17].

1.8 Physical constraints

To reach more realistic results, it is better to use nonlinear constraints like GDB and GRC

1.8.1 Generation rate constraint (GRC)

It is a physical constraint that means a practical limit on the rate of the change in the generating power due to the physical limitations of the turbine. GRC significantly influences realistic power system performance due to its non-linearity characteristic. In practice, the rate of active power change attainable by thermal units has a maximum limit. So, the designed LFC for the unconstrained generation rate situation may not be suitable and realistic. The main reason to consider GRC is that the rapid power increase would draw out excessive steam from the boiler system to cause steam condensation due to adiabatic expansion [18,19].

The GRC of thermal units can be modeled in either the closed-loop or open-loop method. Here, the value of GRC for reheat thermal units is considered as 10% per min, i.e.:

$$|\Delta P| = 0{,}1(\mathrm{Pu/min}) = 0{,}0017(\mathrm{Pu/sec}) \qquad (1.16)$$

Hence, The GRC for the units can be taken into account by adding two limiters, bounded by ±0.0017 within the turbines in the closed loop or open loop method as shown in Figure 1.14 to restrict the generation ramp rate for the thermal plants [15,20].

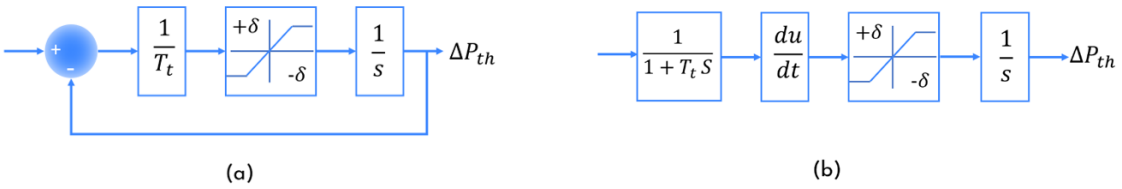

Figure1.14: GRC models (a) Closed Loop modeling, (b) Open Loop modeling

1.8.2 Governor Dead Band (GDB)

Governor Dead Band is defined as the total amount of a continued speed change within which there is no change in valve position. The speed governor dead band has a significant effect on the dynamic performance of the electric energy system. The governor dead band has to be included for a more realistic analysis, which makes the system non-linear. Due to the governor dead band, an increase/decrease in speed can occur before the position of the valve changes. The speed-governor dead band makes the system oscillatory. A describing function approach includes the governor dead band nonlinearity [15].

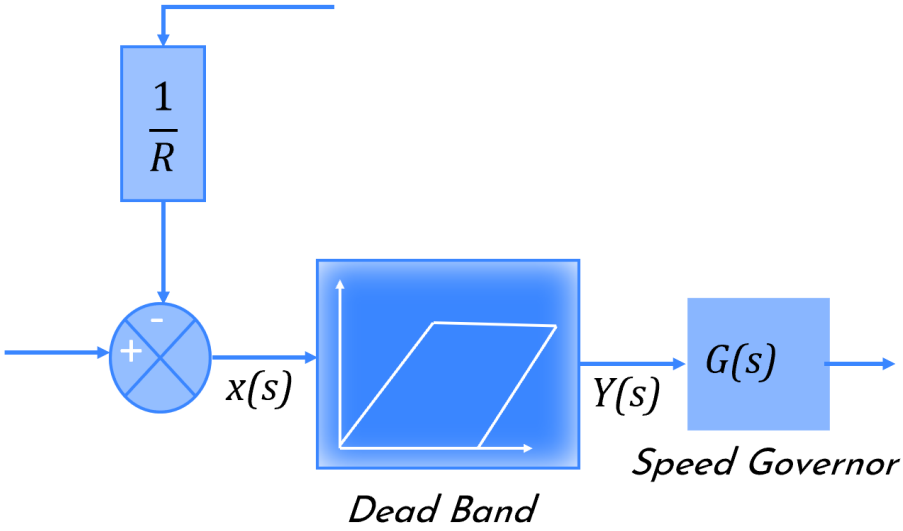

Figure1.15: Block diagram model of speed governor dead-band

1.9 Conclusion

This chapter talks about the connection between load frequency control and automatic generation control. At the start, we have shown power generating units. After that, we have exposed the interconnected power system with block diagrams. Also, some details about PID control with their scheme Then, we have introduced various constraints for studying the power system.

Chapter 2: Wind Power, BESS and Optimization

2.1 Introduction

It was stated that electric power systems exhibit an essential issue for supplying sufficient and reliable electric power with good quality. Consequently, this chapter, firstly, provides the impacts of integrating renewable energy sources on the power system. Also, traditional controllers with their parameters are highlighted. Moreover finally, the generality of meta-heuristics plus the description of this new optimization algorithm called Archimedes optimization algorithm AOA will be discussed.

2.2 What is Renewable Energy?

Renewable energy uses energy sources continually replenished by nature the sun, the wind, water, the Earth's heat, and plants. Renewable energy technologies turn these fuels into usable forms of energy, mainly electricity, heat, chemicals, or mechanical power [21].

2.2.1 Renewable energy resources

Renewable energy (RE) resources are becoming increasingly important in the government's thrust to reduce dependence on fossil fuels and harmful emissions that affect health and the environment. RE includes biomass, geothermal, hydro, wind, solar, and ocean energy which can be converted into more useful energy like electricity. These energy sources are renewable regularly, and their renewal rates are relatively rapid to consider their availability over an indefinite period.

The utilization of RE contributes to the government's strategy to attain a 60 percent self-sufficiency level for total primary energy by 2010. Currently, geothermal, hydro, and biomass resources provide a combined 42 percent share. On the other hand, wind, solar, and micro-hydro resources are getting wide-scale use, particularly for electrification in remote areas [21]

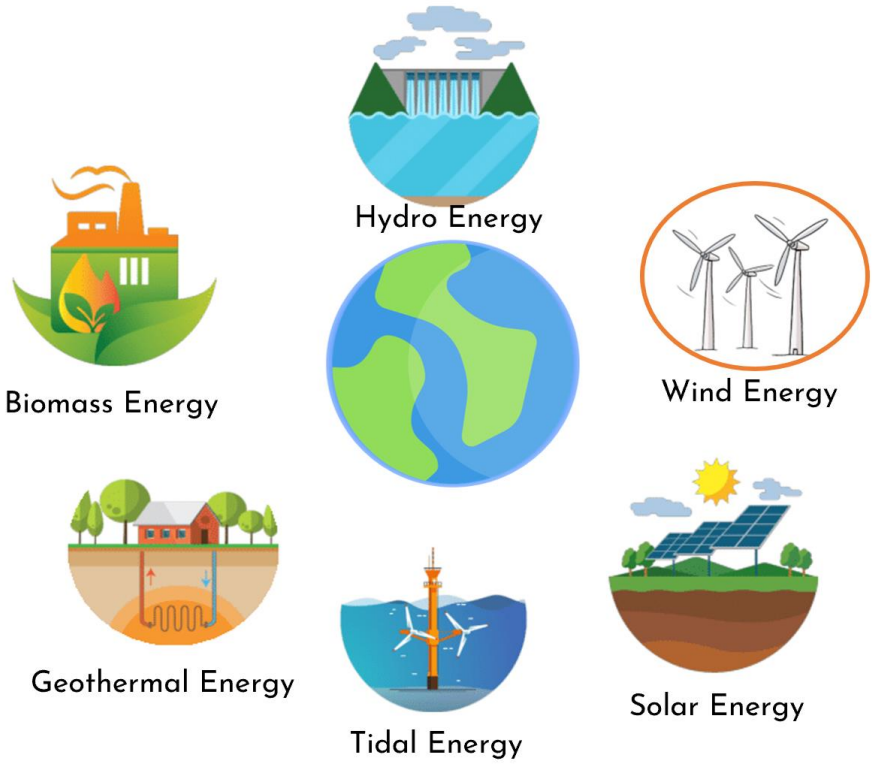

Figure 2.1: Renewable energy sources

2.2.2 Integration of renewable energy sources:

Recently, the increase in renewable energy sources (RESs) utilization in power systems has become inevitable. However, the intermittent energy generations from the RESs cause fluctuation in power system frequency and voltage due to their dependency on weather conditions. These problems may limit the high penetration levels of RESs in power systems. Moreover, RESs employ power electronic converters to integrate and exchange with the grid. These converters lead to lowering the overall system inertia.

Consequently, there will be a lack of frequency/voltage stabilization of the RESs-based power systems compared to conventional synchronous generators-based power systems. Hence, the electrical power system could become unsafe with more RESs installation extensions, increasing their penetration levels. In addition, power systems would be subjected to unbalanced conditions between the energy generation and load demands. These factors

impose several challenges to the frequency control and the existing protection schemes in power systems [22-24].

a. Wind Energy

For hundreds of years, people have used windmills to harness the wind's energy. Today's wind turbines, which operate differently from windmills, are a much more efficient technology. Wind turbine technology may look simply: the wind spins turbine blades around a central hub; the hub is connected to a shaft, which powers a generator to make electricity. However, turbines are highly sophisticated power systems that capture the wind's energy utilizing new blade designs or airfoils. Modern mechanical drive systems, combined with advanced generators, convert that energy into electricity [21].

b. Wind turbine

Power Production of Wind Turbines the aerodynamic power of a wind turbine (WT) can be expressed by equation (2.1). It reflects how much power is possible to extract from the wind. The aerodynamic power is a function of the air density ρ, the wind turbine's rotor area A, the wind speed V and the aerodynamic efficiency Cp. The aerodynamic efficiency can theoretically not exceed the Betz limit of 59%. It can be expressed as a function Cp (λ, θ); hence, it depends on the pitch angle θ and the tip speed ratio λ. Therefore, if the wind turbine enables it, the aerodynamic efficiency can be controlled by adjusting the pitch angle and the rotor speed. Today, the most common control option for wind turbines is pitch control, with other options being stall control and active stall control [25,26].

$$P = \frac{1}{2}\rho A V^3 C_p \tag{2.1}$$

The power production of wind turbines will increase if the rotor area increases and/or if the wind turbine is put in an area with higher wind speeds. The increase in rotor area is seen in the production of wind turbines in the past decades, as illustrated in figure (2.2):

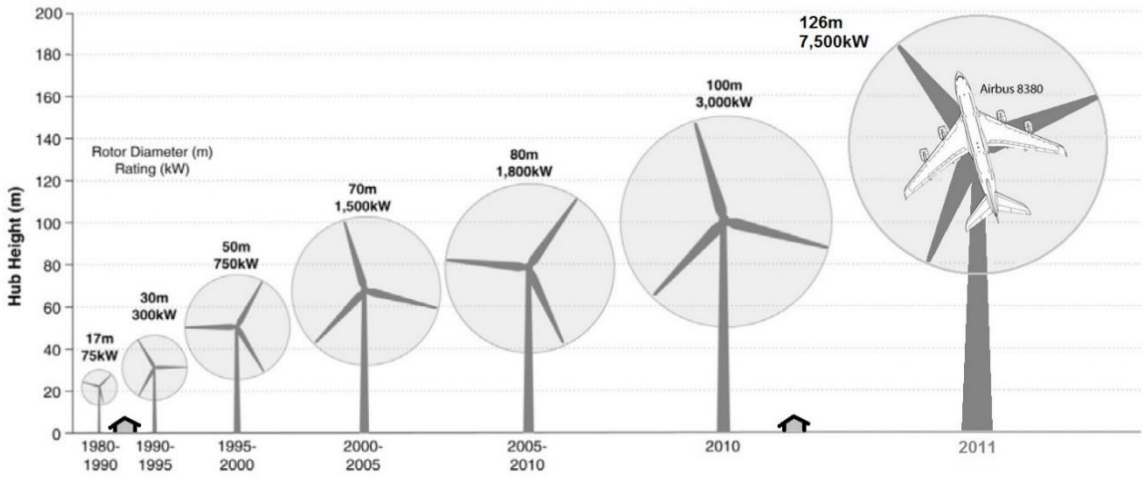

Figure 2.2: Rotor area and hub height of wind turbines since 1980 [25].

c. Impacts of wind power on power systems

Wind power plants affect voltage levels, and power flows in the networks. These effects can benefit the system, mainly when wind power plants are located near load centres and at low penetration levels. For example, wind power plants can support the voltage in the system during fault (low voltage) situations. Also, wind plants with a reactive power control system installed at the end of long radial lines benefit the system since they support the voltage in (usually) low voltage quality parts of the grid. Wind power may need additional transmission and distribution grid infrastructure upgrades, as is the case when any power plant is connected to a grid. In order to connect remote high resource sites, such as offshore or huge wind plants in remote areas, to the load centres, new lines need to be constructed (just as new build pipelines had to be built for oil and gas). In order to maximize the smoothing effects of geographically distributed wind and increase the level of firm power, additional cross-border transmission is necessary to reduce the challenges of managing a system with high levels of wind power. Wind power requires measures for regulating control, just as any other generation technology. Depending on the penetration level and local network characteristics, it affects the efficiency of other generators in the system (and vice versa). In the absence of sufficient intelligent and well-managed power exchange between regions or countries, a combination of (non-manageable) system demands and production may result in situations where wind

generation has to be constrained. Finally, wind power plays a role in maintaining system stability and contributes to the system adequacy and security of supply [27].

2.3 Optimization

Maximizing or minimizing some functions to a set often represents a range of choices available in a given situation. The function allows a comparison of the different choices for determining which may be "best"[28].

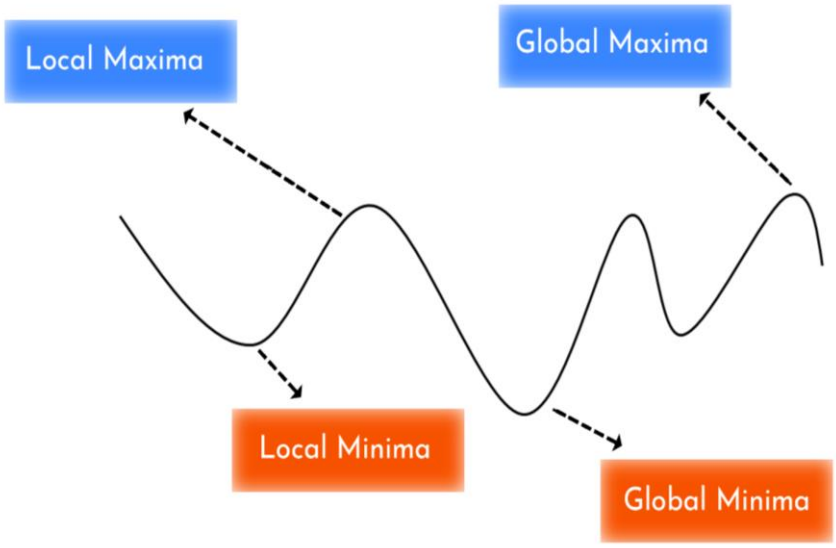

Figure 2.3: Local and Global Optimal Solution

a. Meta-heuristics

Most conventional or classic optimization algorithms are deterministic. These latest used the gradient information; they are called gradient-based algorithms. For example, the well-known one is the Newton-Raphson algorithm, which is gradient-based, using the function values and their derivatives. It works exceptionally well for smooth unimodal problems. However, if there is some discontinuity in the objective function, it does not work well.

For stochastic algorithms, we generally distinguish two types: heuristic and metaheuristic; though their difference is slight, heuristic means 'to find' or' to discover by trial and error.' Quality solutions to a challenging optimization problem can be found in a reasonable amount

of time, but there is no guarantee that optimal solutions are reached. It is good when we do not necessarily want the best solutions but rather reasonable solutions which are easily reachable. Further development over the heuristic algorithms is the so-called meta-heuristic algorithms. Here meta means' beyond' or' higher level,' and they generally perform better than simple heuristics. In addition, all meta-heuristic algorithms use a specific tradeoff of randomization and local search.

It is worth pointing out that no agreed definitions of heuristics and meta-heuristics exist in the literature; some use 'heuristics' and 'meta-heuristics' interchangeably. However, the recent trend tends to name all stochastic algorithms with randomization, and local search are metaheuristics. Here, we will also use this convention. Randomization provides an excellent way to move away from local search to the search on a global scale. Therefore, almost metaheuristic algorithms intend to be suitable for global optimization.

Two significant components of any metaheuristic algorithm are intensification and diversification or exploitation and exploration. Diversification means generating diverse solutions to explore the search space on a global scale. In contrast, intensification means focusing on the search in a local region by exploiting the information that a current good solution is found in this region. This is in combination with the selection of the best solution. The best selection ensures that the solution will converge to the optimality, while the diversification via randomization avoids the solutions being trapped at the local optima and, at the same time, increases the diversity of the solutions. A good combination of these two major components will usually ensure that the global optimality is achievable [31].

2.3.1 Classification

There are many technics of classification, the figure 2.4 below shows their classification

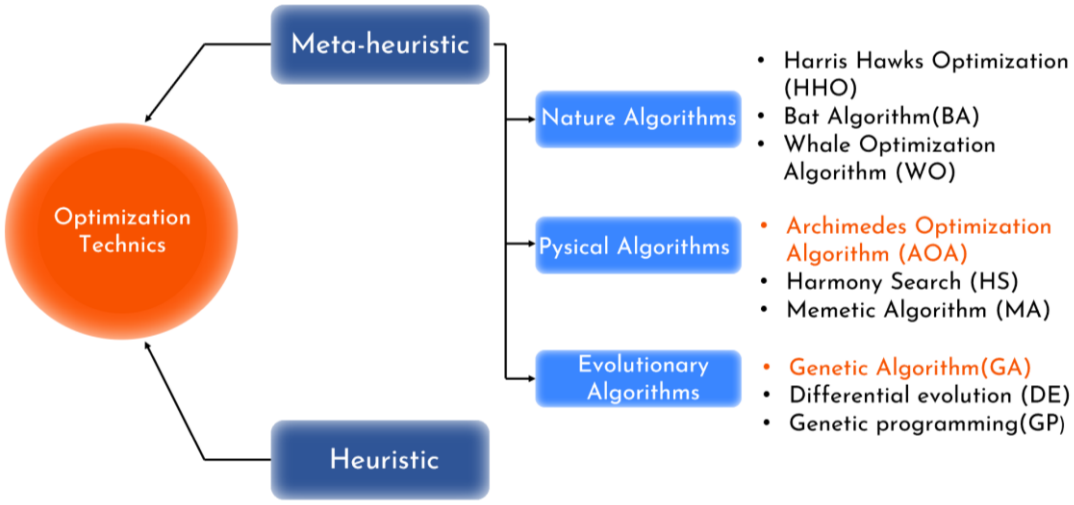

Figure 2.4: Classification of optimization methods

2.3.2 Archimedes' optimization algorithm (AOA)

Archimedes' optimization algorithm (AOA), based on the law of physics known as Archimedes' principle, is proposed to compete with the state-of-the-art and recent optimization algorithms, including other physics-inspired methods. It is worth mentioning that the presented algorithm maintains a balance between exploration and exploitation. This characteristic makes AOA suitable for solving complex optimization problems with many local optimal solutions because it keeps a population of solutions and investigates a large area to find the best global solution [32].

a. Archimedes' principle

Archimedes' principle states that when an object is wholly or partially immersed in a fluid, the fluid exerts an upward force on the object equal to the weight of the fluid displaced by the object. Figure 2.6 show that when an object is immersed in a fluid, it will be experienced by an upward force, called buoyant force, equal to the weight of the fluid displaced by the object [32].

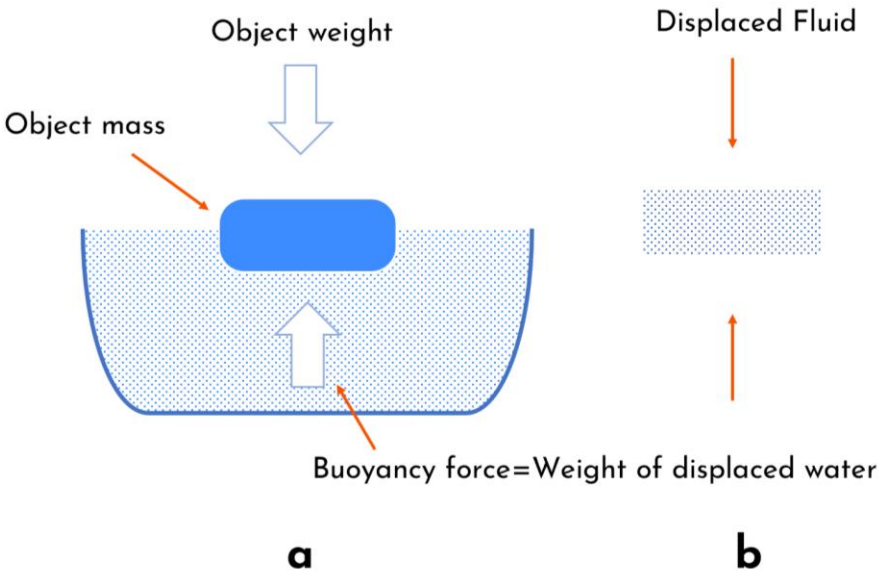

Figure 2.5: (a) An Object is immersed in a fluid, and (b) the volume of fluid displaced

b. Theory

Assume that many objects are immersed in the same fluid Figure 2.7 and each one tries to reach the equilibrium state. The immersed objects have different densities and volumes that cause different accelerations. The object will be in equilibrium if the buoyant force F_b is equal to the object's weight W_o

$$F_b = W_o \tag{2.4}$$

$$\rho_b v_b a_b = \rho_o v_o a_o \tag{2.5}$$

Where ρ is the density, v is the volume, and a is the gravity or acceleration, subscripts b and o are for fluid and immersed objects, respectively. This equation can be rearranged as follows:

$$\frac{\rho_b v_b a_b}{\rho_o v_o} \tag{2.6}$$

Figure 2.6: Many objects immersed in the same fluid

If there is another force influenced on the object like collision with another neighboring object *(r)*, the equilibrium state will be:

$$F_b = W_o \tag{2.7}$$

$$W_b - W_r = W_o \tag{2.8}$$

$$p_b v_b a_b - p_r v_r a_r = p_o v_o a_o \tag{2.9}$$

AOA is a population-based algorithm. In the proposed approach, the population individuals are the immersed objects. Like other population-based metaheuristic algorithms, AOA also commences the search process with an initial population of objects (candidate solutions) with random volumes, densities, and accelerations. Each object is initialized at this stage with its random position in the fluid. After evaluating the fitness of the initial population, AOA works in iterations until the termination condition meets. In every iteration, AOA updates the density and volume of every object. The acceleration of an object is updated based on the condition of its collision with any other neighbouring object. The updated density, volume, and acceleration determine the new position of an object. Following is the detailed mathematical expression of AOA steps [32].

c. Algorithmic steps

In this section, we introduce the mathematical formulation of the AOA algorithm. Theoretically, AOA can be considered a global optimization algorithm is encompassing exploration and exploitation processes. Algorithm presents the pseudo-code of the proposed

algorithm, including population initialization, population evaluation, and updating parameters. Mathematically, the steps of the proposed AOA are detailed as follows [32]:

Step 1—Initialization

Initialize the positions of all objects using equation (2.10):

$$O_i = lb_i + rand \times (ub_i - lb_i); i = 1,2, \dots, N \tag{2.10}$$

where O_i is the *i*-th object in a population of N objects. lb_i and ub_i are the lower and upper bounds of the search-space, respectively. Initialize volume (*vol*) and density (*den*) for each *i*-th object using equation (2.11):

$$\begin{aligned} \text{den}_i &= \text{rand} \\ \text{vol}_i &= \text{rand} \end{aligned} \tag{2.11}$$

where *rand* is a *D* dimensional vector randomly generates number between [0, 1]. And finally, initialize acceleration (*acc*) of *i-th* object using equation (2.12):

$$acc_i = lb_i + rand \times (ub_i - lb_i) \tag{2.12}$$

In this step, evaluate initial population and select the object with the best fitness value. Assign x_{best} , den_{best} , vol_{best} , and acc_{best}.

Step 2—Update densities, volumes

The density and volume of object *i* for the iteration *t + 1* is updated using equation (2.13):

$$\begin{aligned} den_i^{t+1} &= den_i^t + \text{rand} \times (\text{ den }_{best} - den_i^t) \\ vol_i^{t+1} &= vol_i^t + \text{rand} \times (vol_{best} - vol_i^t) \end{aligned} \tag{2.13}$$

where vol_{best} and den_{best} are the volume and density associated with the best object found so far, and *rand* is uniformly distributed random number.

Step 3—Transfer operator and density factor

In the beginning, collision between objects occurs and, after a period of time, the objects try to reach at equilibrium state. This is implemented in AOA with the help of transfer

operator *TF* which transforms search from exploration to exploitation, defined using equation (2.14):

$$TF = \exp\left(\frac{t-t_{max}}{t_{max}}\right) \tag{2.14}$$

where transfer *TF* increases gradually with time until reaching 1. Here *t* and t_{max} are iteration number and maximum iterations, respectively. Similarly, density decreasing factor *d* also assists AOA on global to local search. It decreases with time using equation (2.15):

$$d^{t+1} = \exp\left(\frac{t_{\max}-t}{t_{max}}\right) - \left(\frac{t}{t_{max}}\right) \tag{2.15}$$

where d^{t+1} decreases with time that gives the ability to converge in already identified promising region. Note that proper handling of this variable will ensure balance between exploration and exploitation in AOA.

Step 4.1—Exploration phase (collision between objects occurs)

If $TF \leq 0.5$, collision between objects occurs, select a random material (*mr*) and update object's acceleration for iteration *t + 1* using equation (2.16):

$$\mathrm{acc}_i^{t+1} = \frac{den_{mr}+vol_{mr}\times acc_{mr}}{den_i^{t+1}\times \mathrm{vol}_i^{t+1}} \tag{2.16}$$

where den_i, vol_i, and acc_i are density, volume, and acceleration of object *i*. Where as acc_{mr}, den_{mr}, and vol_{mr}, are the acceleration, density, and volume of random material. It is important to mention that $TF \leq 0.5$ ensures exploration during one third of iterations. Applying value other than 0.5 will change exploration-exploitation behavior.

Step 4.2—Exploitation phase (no collision between objects)

If $TF \leq 0.5$, there is no collision between objects, update object's acceleration for iteration *t + 1* using equation (2.17):

$$acc_i^{t+1} = \frac{\mathrm{den}_{\mathrm{best}} + \mathrm{vol}_{\mathrm{best}} \times \mathrm{acc}_{\mathrm{best}}}{\mathrm{den}_i^{t+1}\times \mathrm{vol}_i^{t+1}} \tag{2.17}$$

where acc_{best} is the acceleration of the best object.

Step 4.3—Normalize acceleration

Normalize acceleration to calculate the percentage of change using equation (2.18):

$$acc_{i-norm}^{t+1} = u \times \frac{acc_i^{t+1} - min(acc)}{max(acc) - min(acc)} + l \quad (2.18)$$

where u and l are the normalization range and set to 0.9 and 0.1, respectively, the acc_{i-norm}^{t+1} determines the percentage of steps each agent will change. If object i is far away from the global optimum, the acceleration value will be high—meaning that the object will be in the exploration phase; otherwise, in the exploitation phase, this illustrates how the search transforms from exploration to exploitation phase. In the usual case, the acceleration factor begins with a significant value and decreases with time; This helps search agents move towards the global best solution, and at the same time, they move away from local solutions. However, it is noteworthy to mention that there may remain a few search agents that need more time to stay in the exploration phase than in normal case. Hence, AOA achieves the balance between exploration and exploitation.

Step 5—Update position

If $TF \leq 0.5$ (exploration phase), the i^{th} object's position for next iteration $t + 1$ using (2.19):

$$x_i^{t+1} = x_i^t + C_1 \times \text{ rand } \times acc_{i-\text{ norm}}^{t+1} \times d \times (x_{\text{rand}} - x_i^t) \quad (2.19)$$

where C_1 is constant equals to 2. Otherwise, if $TF \leq 0.5$ (exploitation phase), the objects update their positions using equation (2.20):

$$x_i^{t+1} = x_{\text{best}}^t + F \times C_2 \times \text{ rand } \times acc_{i-norm}^{t+1} \times d \times (T \times x_{\text{best}} - x_i^t) \quad (2.20)$$

where $C_2$is a constant equal to 6. T increases with time and it is directly proportional to transfer operator and it is defined using $T = C_3 \times TF$. T increases with time in range [$C_3 \times$ 0.3, 1] and takes a certain percentage from the best position, initially. It starts with low percentage as this results in large difference between best position and current position, consequently step-size of random walk will be high. As the search proceeds, this percentage increases gradually to decrease difference between the best position and the current position. This leads to achieving an appropriate balance between exploration and exploitation.

F is the flag to change the direction of motion using equation (2.21):

$$F = \begin{cases} +1 \text{ if } P \leq 0.5 \\ -1 \text{ if } P > 0.5 \end{cases} \quad (2.21)$$

where $P = 2 \times \text{ rand } - C_4$.

Step 6—Evaluation

Evaluate each object using objective function f and remember the best solution found so far. Assign x_{best} , den_{best} , vol_{best} , and acc_{best} .

Algorithm: Pseudo code of AOA.

Procedure AOA (population size N, maximum iterations t_{max} ,C_1 ,C_2,C_3,and C_4)

Initialize objects population with random positions, densities and volumes using (2.10), (2.11), and (2.12), respectively.

Evaluate initial population and select the one with the best fitness value.

Set iteration counter *t=1*

While $t \leq t_{max}$ **do**

for each object *i* **do**

update density and volume of each object using (2.13)
update transfer and density decreasing factors *TF* and *d* using (2.14) and (2.15), respectively.

If $TF \leq 0.5$ **then** ➢ Exploration phase

Update acceleration using (2.16) and normalize acceleration using (2.18)

Update position using (2.19)

else ➢ Exploitation phase

Update acceleration using (2.17) and normalize acceleration using (2.18)

Update direction flag *F* using (2.21)

Update position using (2.20)

end if

end for

Evaluate each object and select the one with the best fitness value.

Set *t= t+1*

end while

return object with best fitness value.

end procedure

2.3.3 Optimization of Regulator Parameters

In control system design and analysis, certain design specifications are required to reduce the steady-state error of the system. The optimum value of controller parameters is obtained by minimizing a specified objective function [29,30]. There are many criteria used in the controller synthesis procedure. The flowchart of Figure 2.4 presents the different performance criteria used for the controller synthesis.

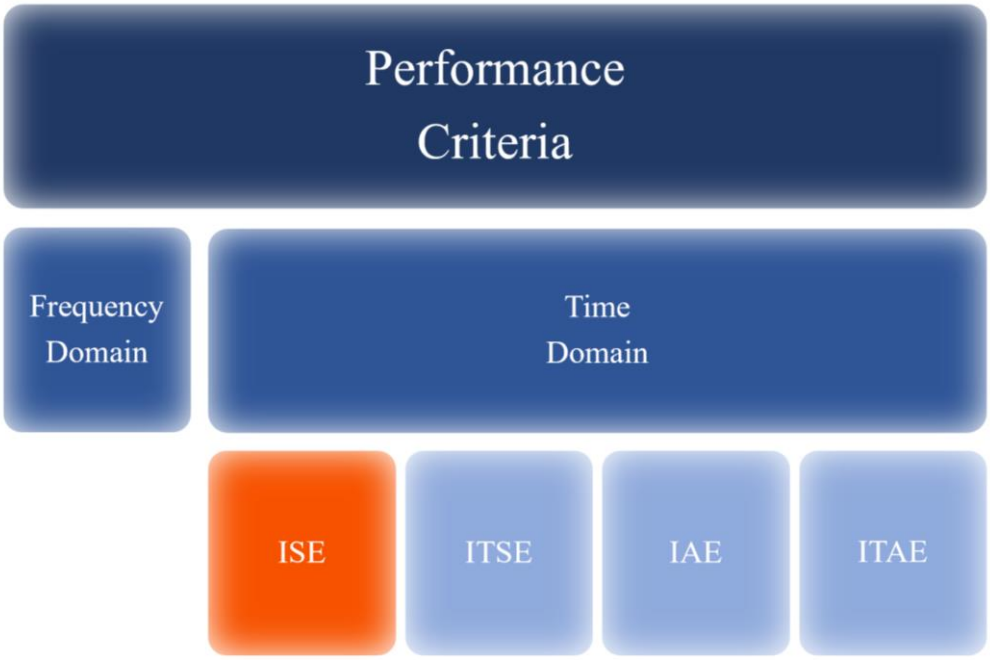

Figure 2.7: Different Existing performance Criteria

a. Integral of Square Error:

For the performance evaluation of PID controllers, the ISE performance index is used. Its function is described by equation (2.2) as follows:

$$J = ISE = \int_0^\infty e^2(t)dt \tag{2.2}$$

Here, the error which is needs to be minimized is $e(t)$.For n areas power system, the error $e(t)$ is represented by:

$$e(t) = \sum_{i=1}^{n} ACE_i \tag{2.3}$$

2.4 Battery Energy Storage System (BESS)

A Battery Energy Storage System (BESS) is a type of energy storage device that uses batteries as its underlying storage technology. A battery energy storage system is more than just a battery and requires additional components that allow the battery to be connected to an electrical network. A *bidirectional inverter* is the main device that converts power between the AC line voltage and the DC battery terminals and allows power to flow both ways to charge and discharge the battery. Other components of a BESS may include an isolation transformer, protection devices (e.g., circuit breakers), cooling systems, and a high-level control system to coordinate the operation of all components in the system [33].

2.4.1 Benefits of BESS

There are many benefits of BESS, and we will mention them in the following [34]:

- Energy storage is one of the ways to deal with the variability of renewable resources;
- Energy storage devices can harvest excess energy during periods of low demand and inject the stored energy when needed during peak usage periods;
- Providing extra energy in case of power system contingencies or a rapid change in demand;

2.4.2 Modelling of BESS

The first-order transfer function model of BESS is given in Figure 2.8:

Figure 2.8: BESS First Order Transfer Function model

The BESS can be represented in LFC as:

$$\Delta P_{BESS} = \Delta f \frac{K_{BESS}}{1+sT_{BESS}} \tag{2.22}$$

The BESS can be either in charging mode or discharging mode based on the system frequency as shown in Table 2.2 [35]

Table 2.2: Battery charging status based on system Frequency

Δf	**BESS Statue**
Positive	Charging
Negative	Discharging

2.5 Conclusion:

This chapter explains renewable energy resources and their impact on the power system. Firstly, the power production of the wind turbine was briefly discussed. The next step is to define the optimization and classify the meta-heuristics. After that, we have provided different performance criteria that can be applied to optimize regulator parameters. Then, a novel AOA method is explained in detail. Finally, we provide BESS and some benefits from BESS.

Chapter 3: Simulation and Results

3.1 Introduction

This chapter will show how successful Battery Energy Storage System (BESS) is in solving the LFC problem with wind power integration. The tests are carried out in a three-area reheat system, where GDB and GRC are taken into account for a more realistic case study. ISE uses a new optimization algorithm called AOA to discover the best PID settings for LFC. The performance of the new algorithm AOA is then compared to that of other Evolutionary Algorithms, such as the Genetic Algorithm (GA).

3.2 The problem's Formulation

In our case, the Objective Function is given by the following equation:

$$J = ISE = \int_0^t \{ACE_1^2 + ACE_2^2 + ACE_3^2\}dt \tag{3.1}$$

The main settings of the PID controller have to be tuned using optimization algorithms by minimizing dynamical criteria. In our study, the optimization problem can be formulated as follows:

Minimize $J(k_p,k_I,k_D)$

$$\text{subjected to } \begin{cases} K_P^{min} \le K_P \le K_P^{max} \\ K_I^{min} \le K_I \le K_I^{max} \\ K_D^{min} \le K_D \le K_D^{max} \end{cases} \tag{3.2}$$

k_p,k_I and k_D are the three tunable controller parameters. In this study, the gain bounds limits are fixed between 0 and 10. The parameters of GA and AOA are presented in Table 3.1; the standard settings include population size (N = 30), and maximum iterations (T = 150).

Table 3.1: Parameter Settings of GA and AOA

Algorithms	Parameters
GA	Population size=30 Number of iterations=150 Crossover=20, probability=0.8 Mutation=20, probability=0.2
AOA	Objects Number=30 Number of iterations =150 C_1=2, $C_2 = 6$ $C_3 = 2, C_4 = 0.5$

3.3 Investigated power system

The system of our study case involves a three-area interconnected thermal power system with the presence of a wind turbine, as presented in Figure 3.1. Each area comprises a governing speed system, turbine, generator, GDB, and GRC. The nominal system and wind parameters are offered in ***Appendix A***.

First, we consider 1% load variation in area 1 ($\Delta P_{L1} = 1\%$ p.u.) . After that, we consider wind turbine load variation in area1.

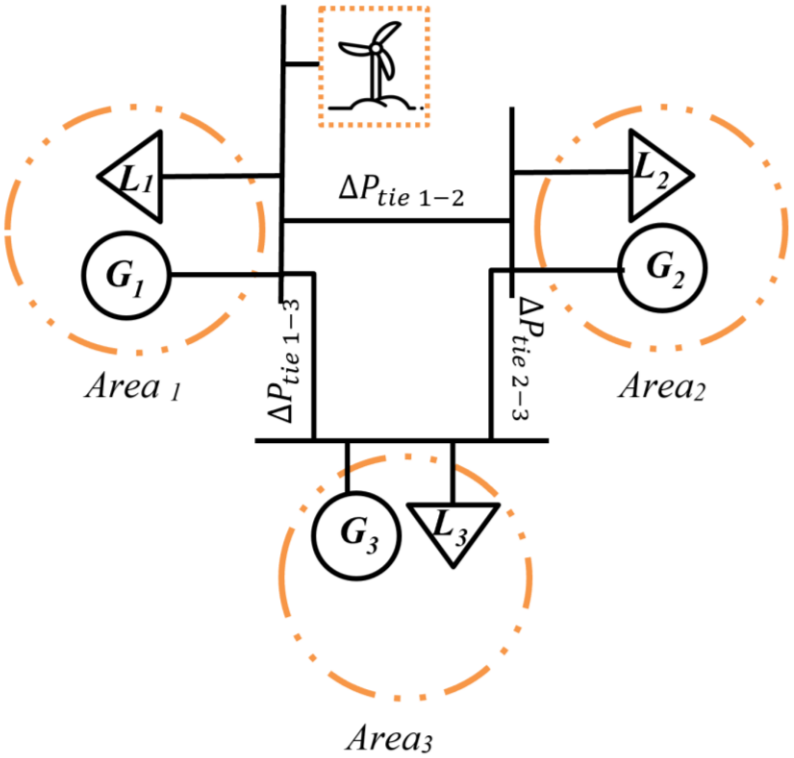

Figure 3.1: Three areas LFC test system with integration of wind power

3.4 Cases Study

In this study, simulations have been performed by MATLAB/SIMULINK on the three areas reheat thermal system. According to a wind turbine in area 1.

3.4.1 Case-1

Three areas reheat Thermal system, step load disturbance in area 1, using GA and AOA algorithms.

The GA and AOA algorithms are executed to define the optimum controller's parameters by evaluating ISE criteria. After the optimization process, the optimal controller's settings are tabulated in Table 3.2 and Table 3.3, respectively. The frequency dynamical response according to the first area without any constraints, with each constraint alone and with all non-linear constraints, is presented in Figure 3.3.

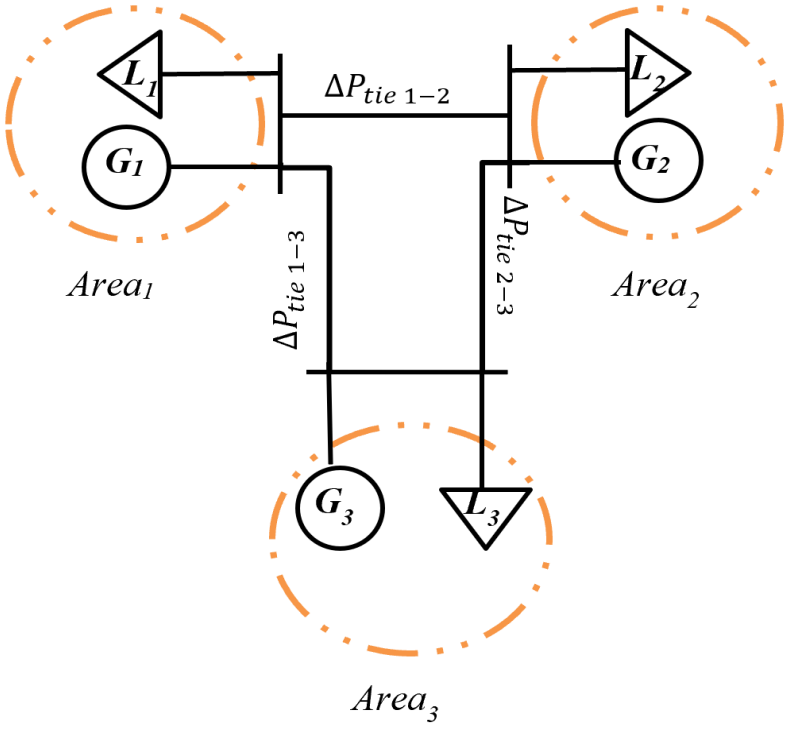

Figure 3.2: Three areas LFC test System with 1% Load variation in area 1

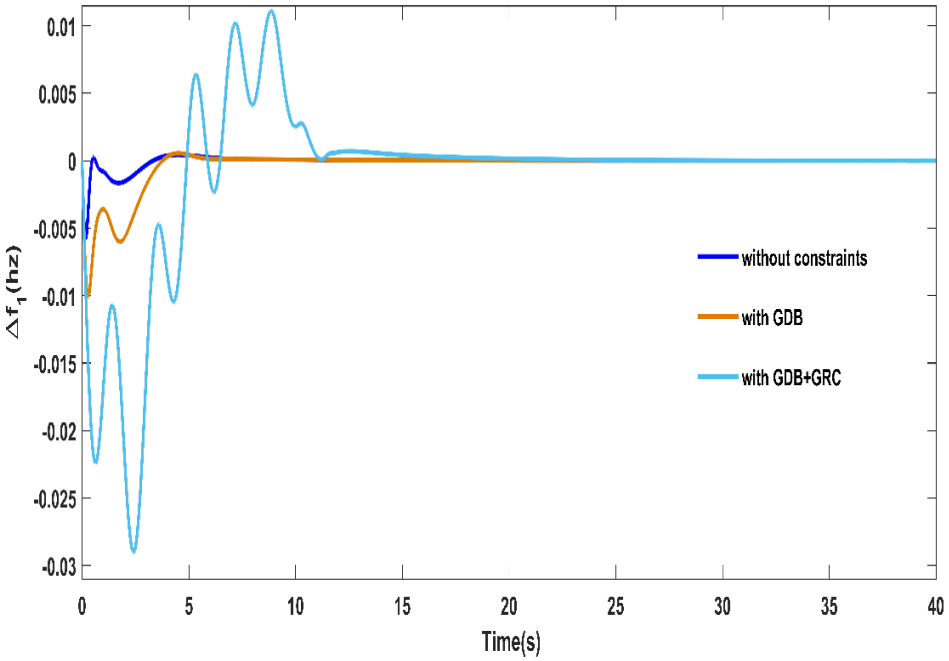

Figure 3.3: Frequency dynamical response of the first area with and without the different constraints

Table 3.2: Optimal controller's settings using ISE criterion (GA)

Controller's gains	K_p	K_I	K_D
Area 1	7.0024	9.7611	2.7469
Area 2	8.7933	9.9890	3.7308
Area 3	9.8707	9.9887	4.2410
Objective function: 0.2434			

Table 3.3: Optimal controller's settings using ISE criterion (AOA)

Controller's gains	K_p	K_I	K_D
Area 1	6.2837	9.0190	2.5432
Area 2	10.0000	8.3542	3.4147
Area 3	8.9651	9.8342	3.0416
Objective function: 0.2409			

In addition, to confirm the effectiveness of the new algorithm AOA used in our system, AOA was compared with another optimization algorithm such as Genetic Algorithm (GA), as shown in Figure 3.4. Both optimization methods (AOA and GA) were applied using the ISE criterion to the same investigated power system.

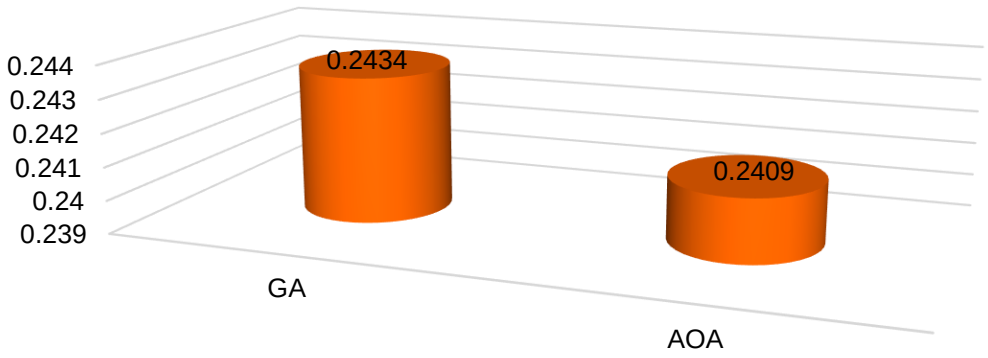

Figure 3.4: Comparison between AOA and GA using ISE criterion

Figure 3.4 shows that AOA is a better optimization than GA since the AOA value was lowered by 1.03% when compared to the value obtained by GA.

3.4.2 Case-2

Three areas reheat thermal system with integration Wind Power in area1 see Figure3.5.

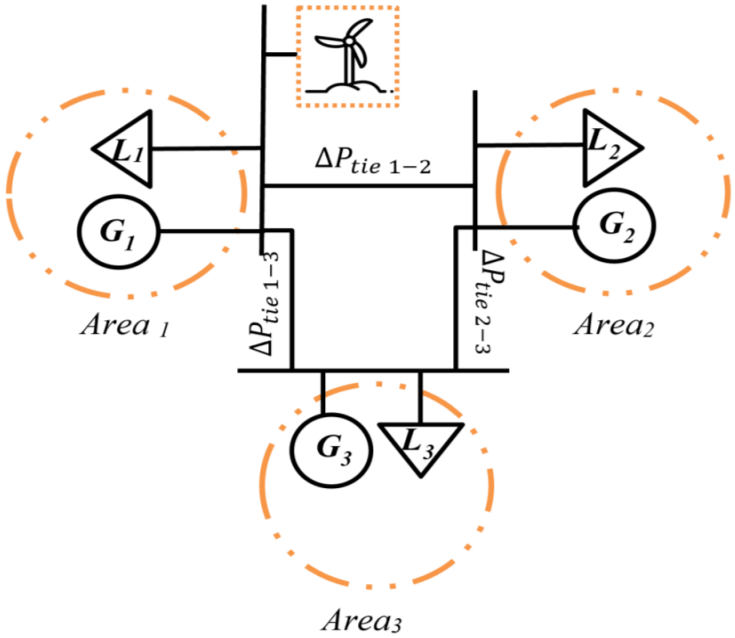

Figure 3.5: Three areas LFC system With Power Wind

The dynamic response of the system obtained has been presented in figure 3.6.

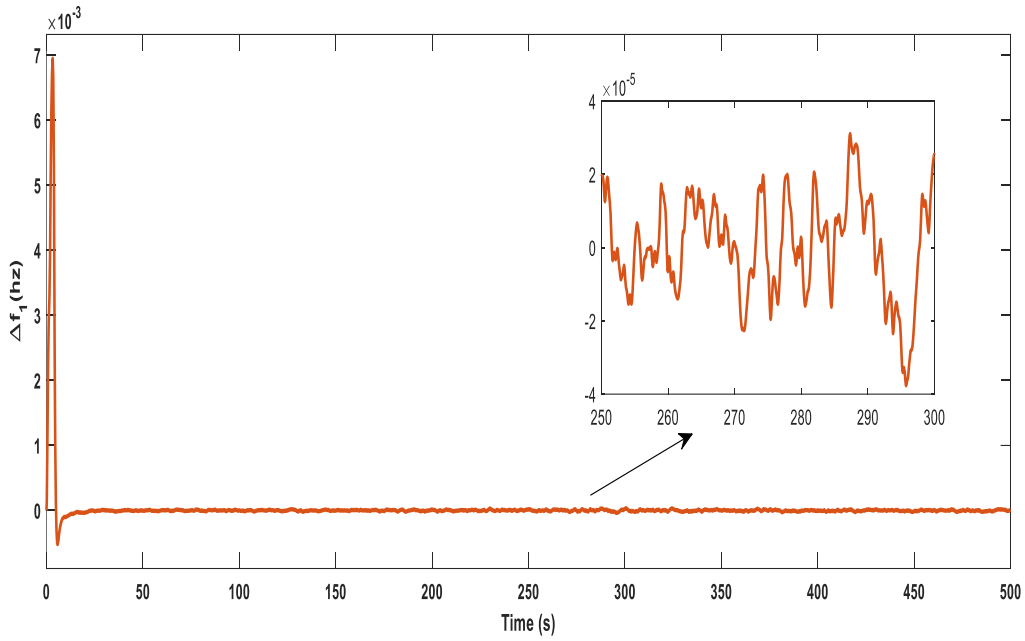

Figure 3.6: Dynamical response of frequency deviation area 1 with Wind Power

The integration of wind power in the power system creates a problem of frequency instability due to random wind speed, which makes the power output of the rotor unexpected and random. It is a problem for power system stability.

Plus, it suffers from high-frequency overshoot at the connection of the wind generation.

3.4.3 Case-3

Three areas reheat thermal system with step load disturbance in area 1, a battery type BESS installed in all three areas.

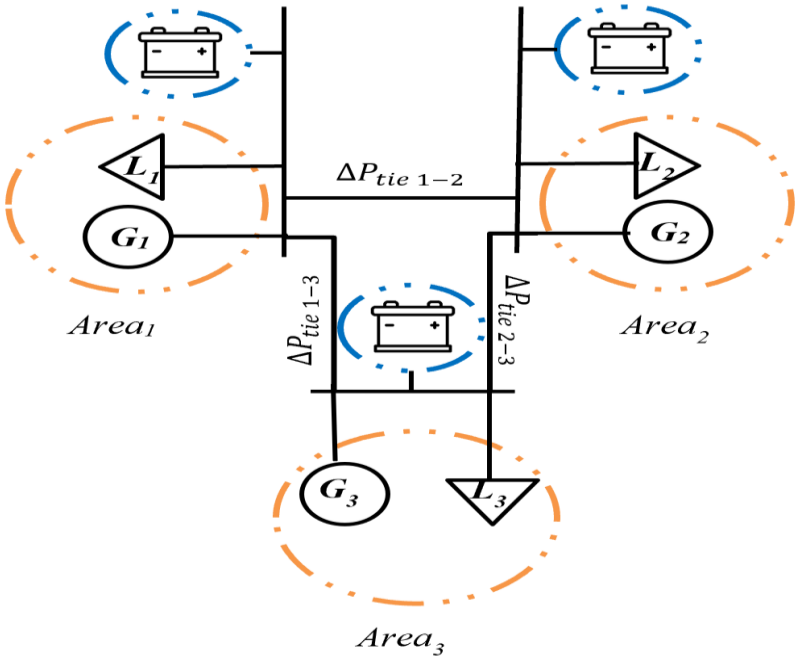

Figure 3.7: Three areas LFC System with BESS

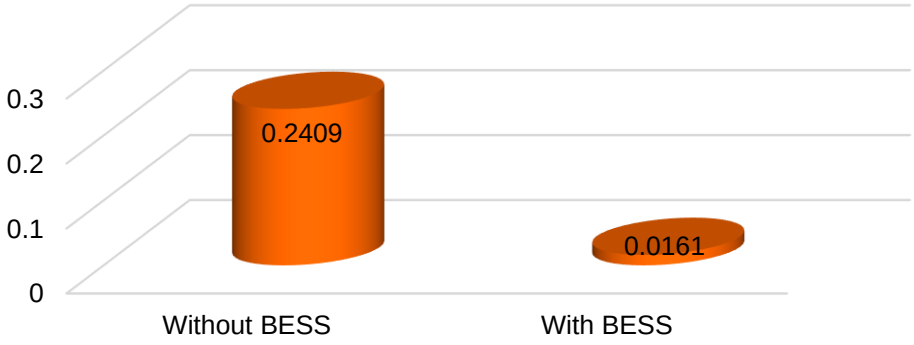

Figure 3.8: Comparison of system without BESS, with BESS of ISE value

We can notice from Figure 3.8 that the value of ISE with BESS was reduced compared to the value of ISE without BESS.

As well Figures 3.9 (a, b and c) displays respectively dynamical responses of frequency deviation in area 1 (Δf_1), Area Control Error (ACE_1), mechanical power deviation (ΔP_{m1}) and tie line power deviation (ΔP_{tie13}) respectively.

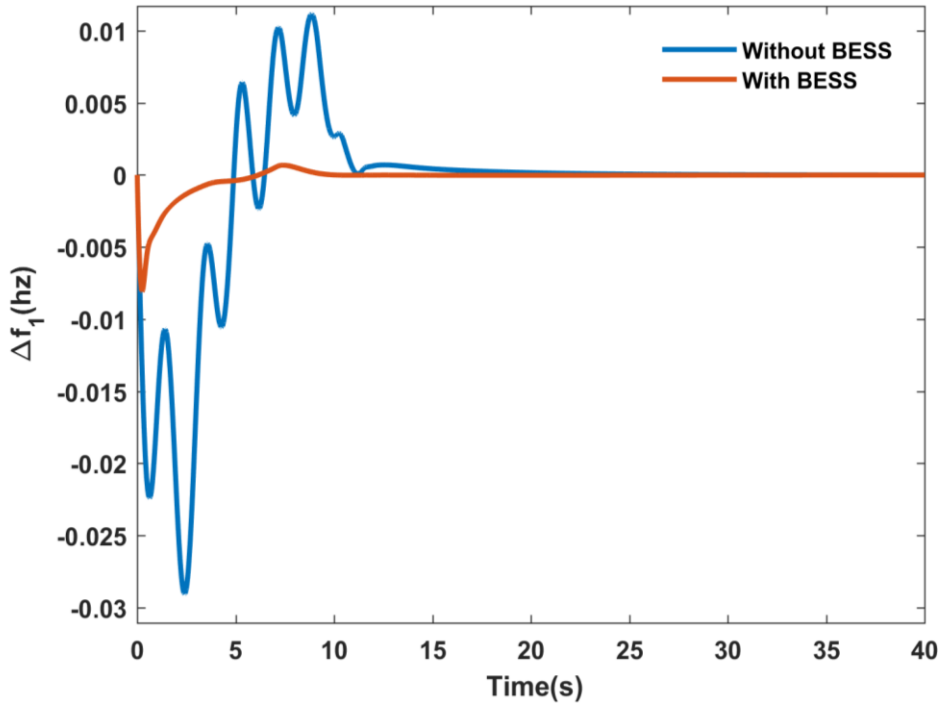

(a)

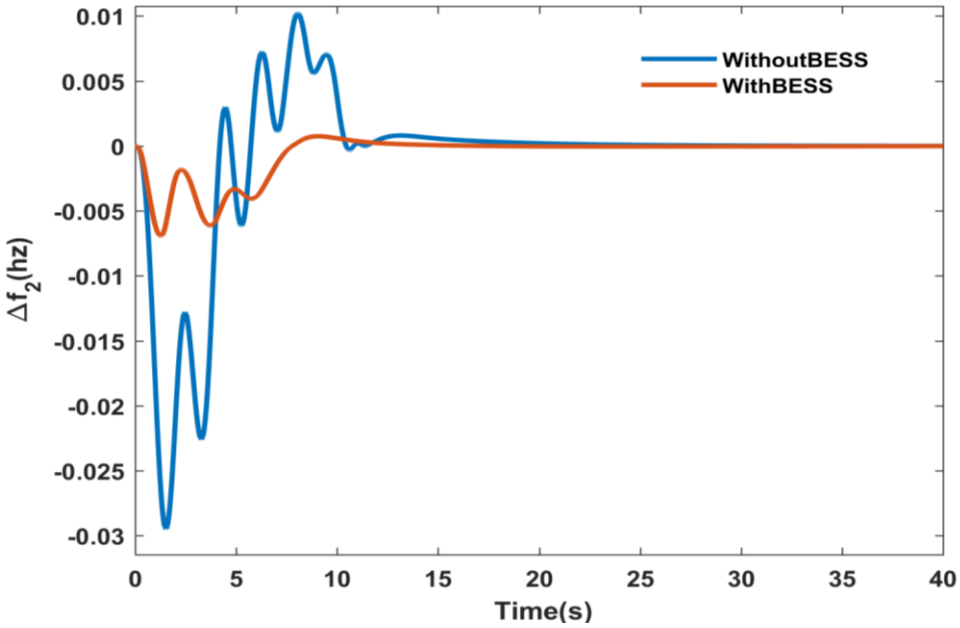

(b)

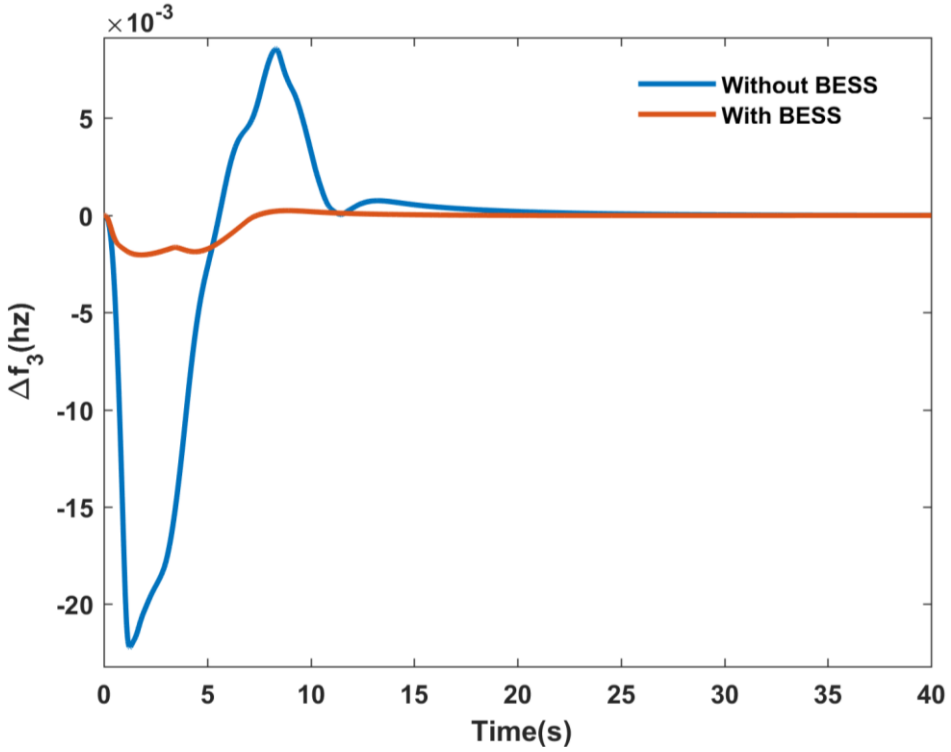

(c)

Figures 3.9: Dynamic response of (a): Δf_1, (b): Δf_2 and (c): Δf_3 with and without BESS

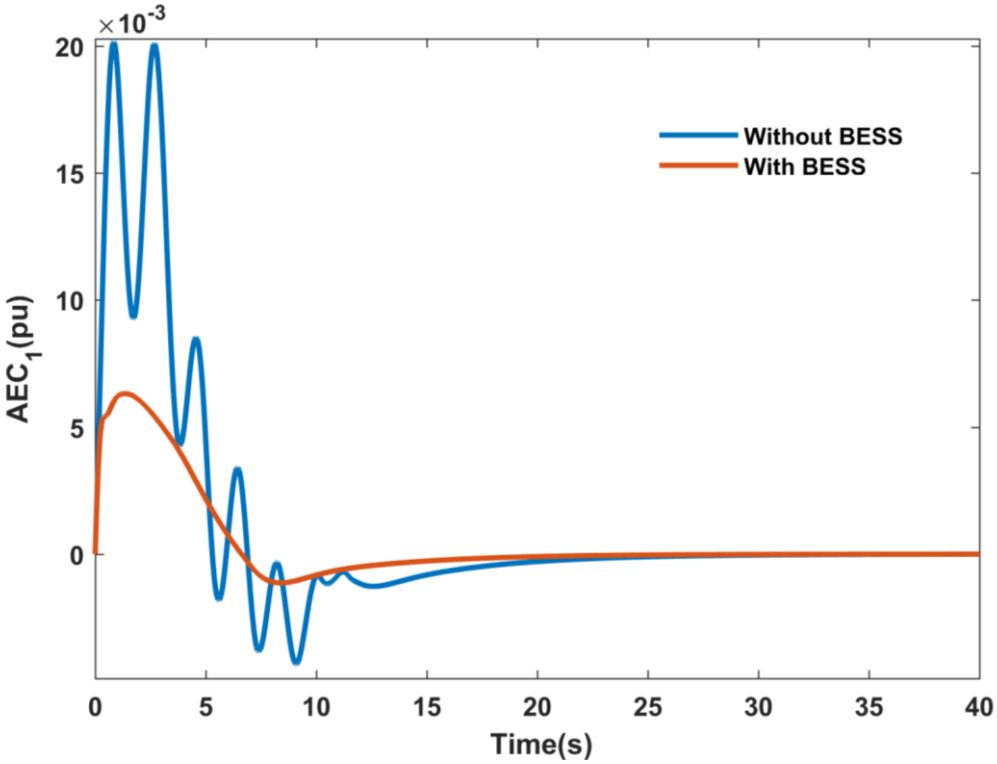

(a)

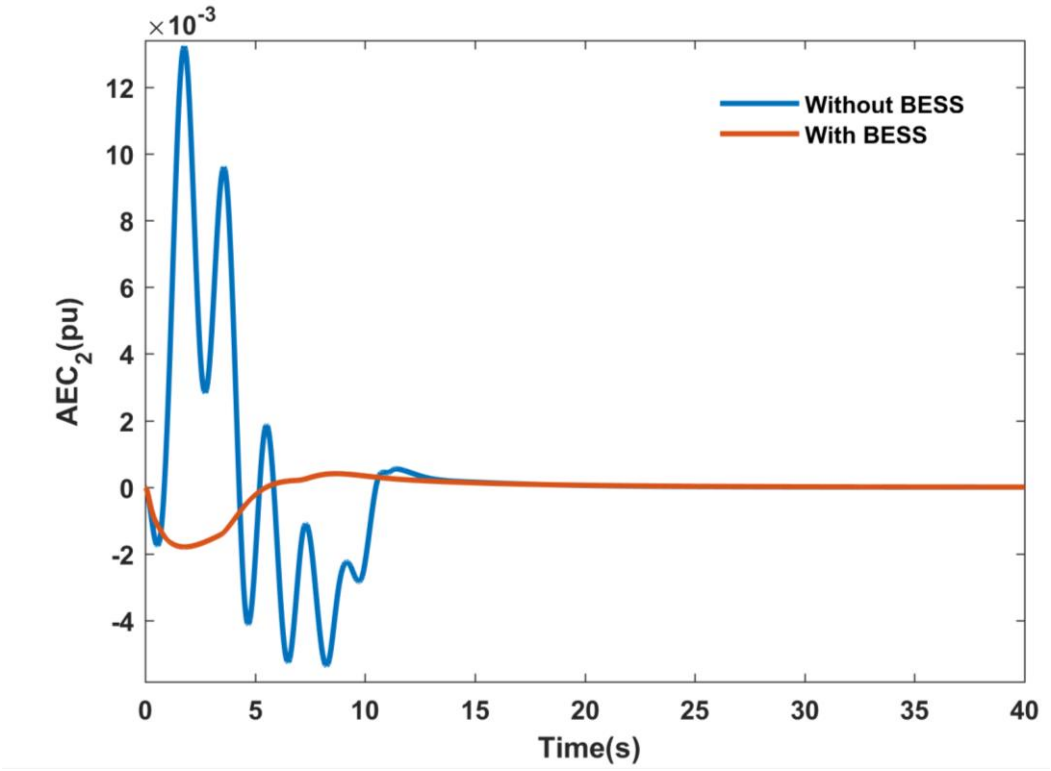

(b)

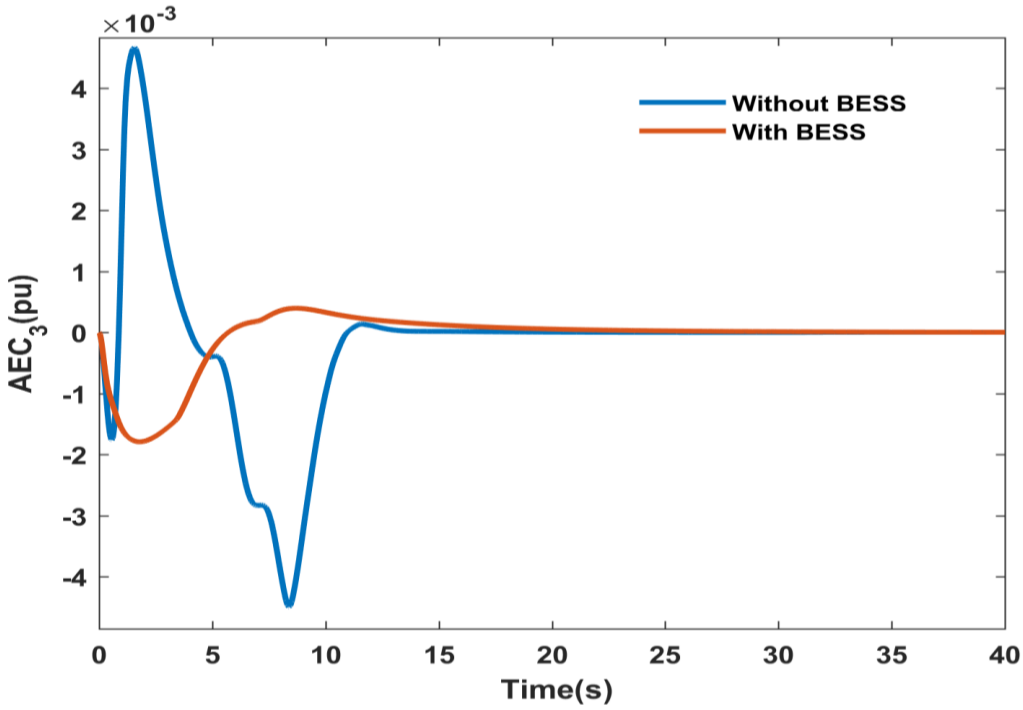

(c)

Figures 3.10: Dynamic response of (a): ACE_1, (b): ACE_2 and (c): ACE_3 with and without BESS

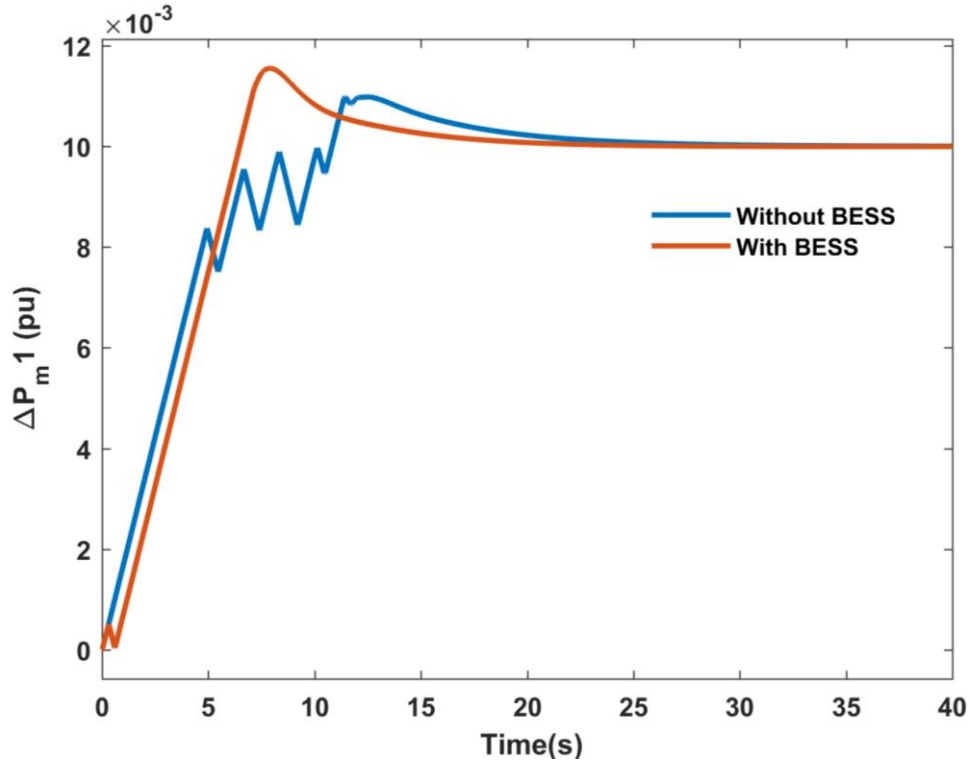
×10^-3
12
10
8
6
4
2
0
ΔP_m1 (pu)
0
5
10
15
20
25
30
35
40
Time(s)
Without BESS
With BESS

(a)

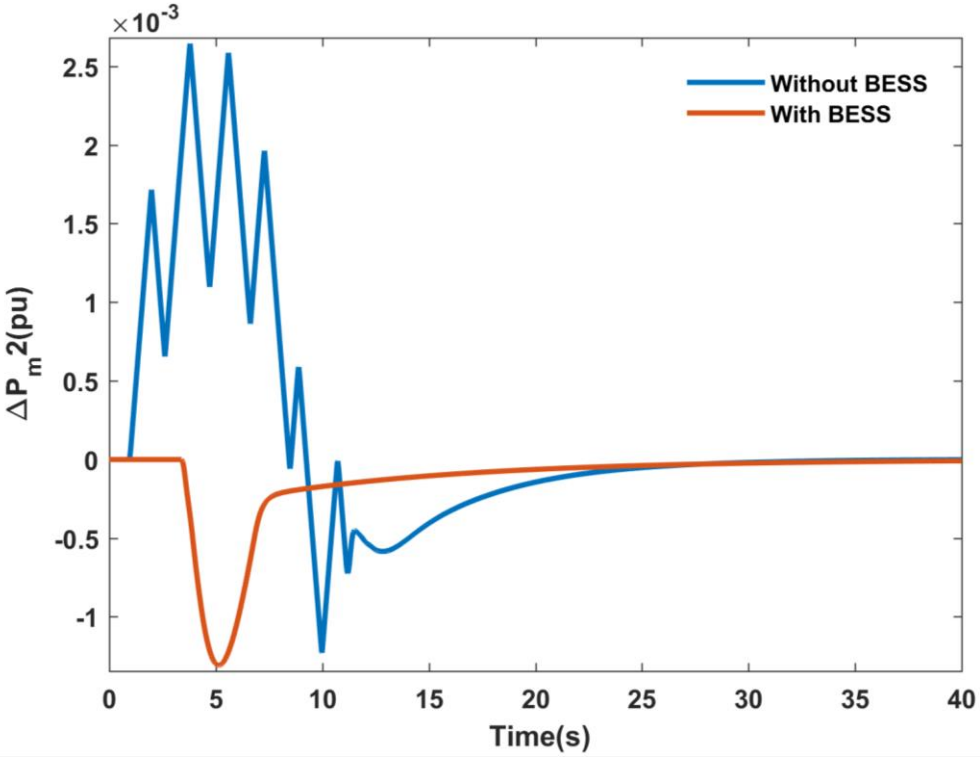
×10^-3
2.5
2
1.5
1
0.5
0
-0.5
-1
ΔP_m2(pu)
0
5
10
15
20
25
30
35
40
Time(s)
Without BESS
With BESS

(b)

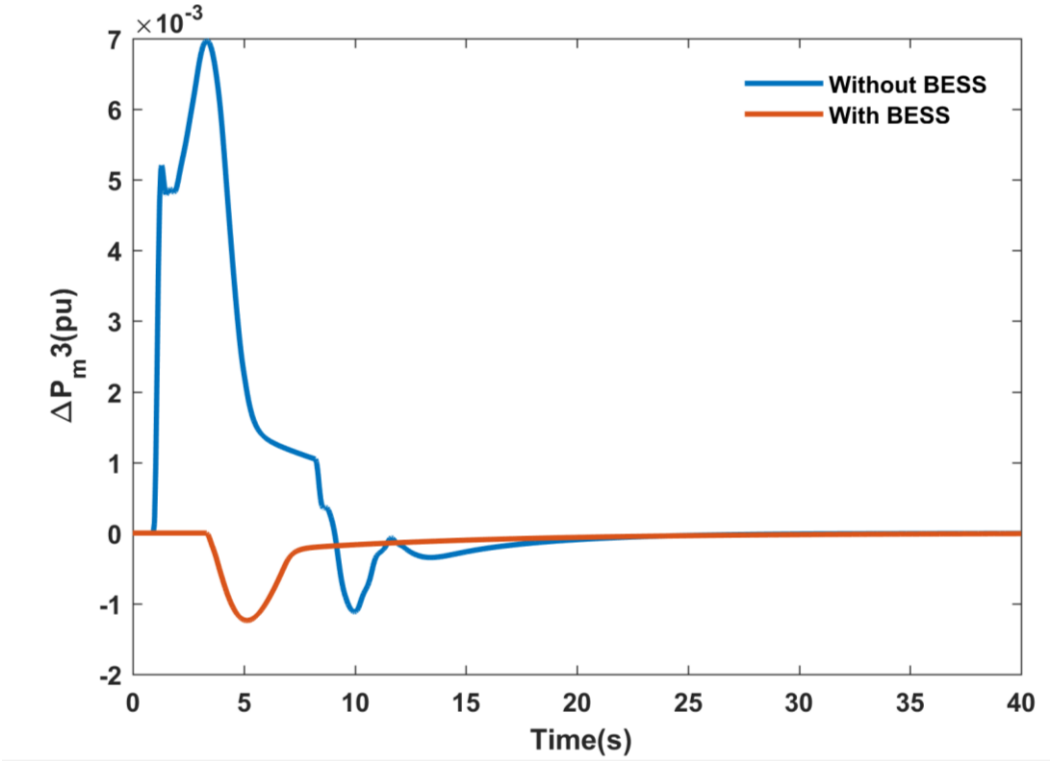

(c)

Figures 3.11: Dynamic response of (a): ΔP_{m1}, (b): ΔP_{m2} and (c): ΔP_{m3}

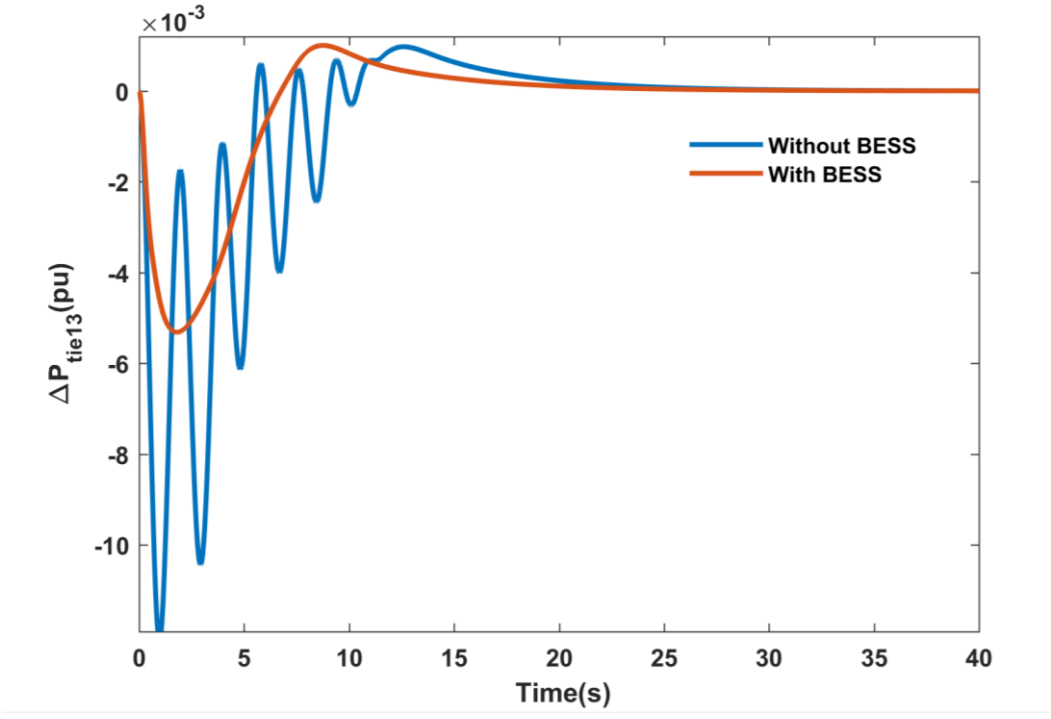

(a)

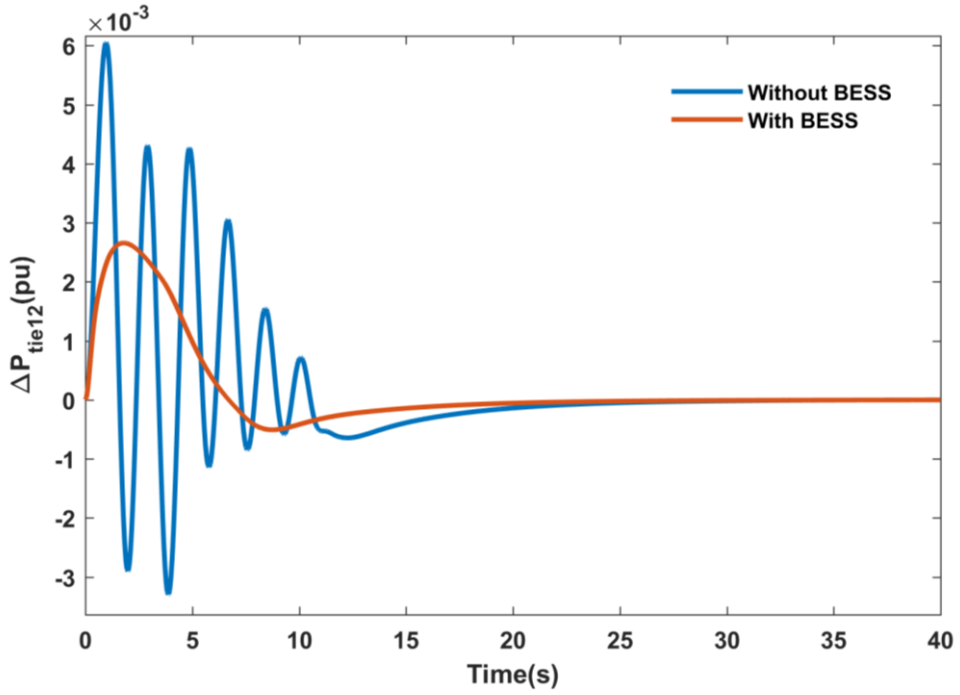

(b)

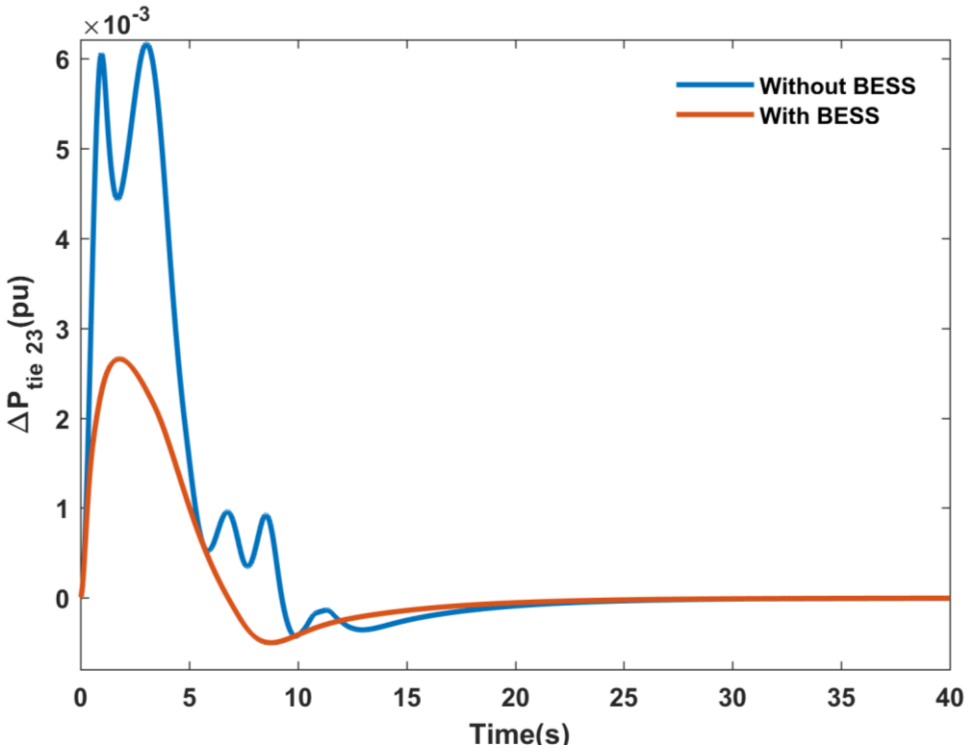

(c)

Figures 3.12: Dynamic response of (a): ΔP_{tie13}, (b): ΔP_{tie12} and (c): ΔP_{tie23}

It is clear from these results that the system with BESS performed far better than the one without BESS.

Table 3.4: Settling Time and Peak Overshoot/Undershoot for Case-3

		S.T(s)	P.O	P.U
Δf1	Without BESS	13.7089	$1.115*10^{-2}$	$-2.905*10^{-2}$
	With BESS	9.0117	$6.769*10^{-4}$	$-8.092*10^{-3}$

It is clear from Table 3.4 that the peak overshoot/undershoot and Settling Time with BESS is smaller as against without BESS.

3.4.4 Case-4

Figure 3.14 shows three areas of reheat thermal system with Wind Power in area1 and BESS installed in all areas.

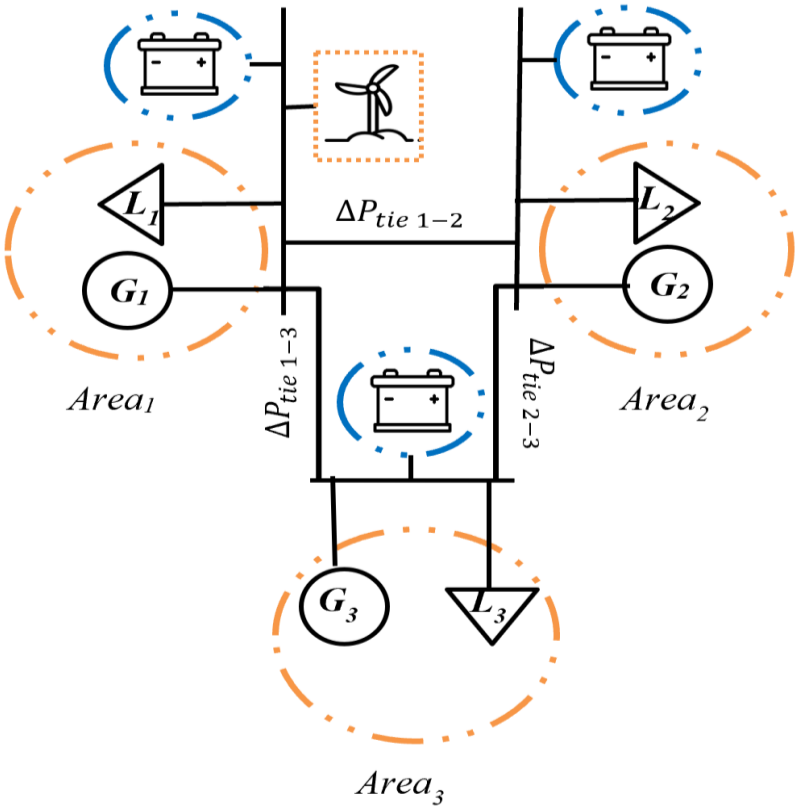

Figure 3.13: Three areas LFC test system with wind power and BESS.

Figure 3.14 and Figure 3.15 show that the proposed BESS in all 3 areas can provide satisfactory performance in restoring system frequency against various disruptions produced by wind power integration.

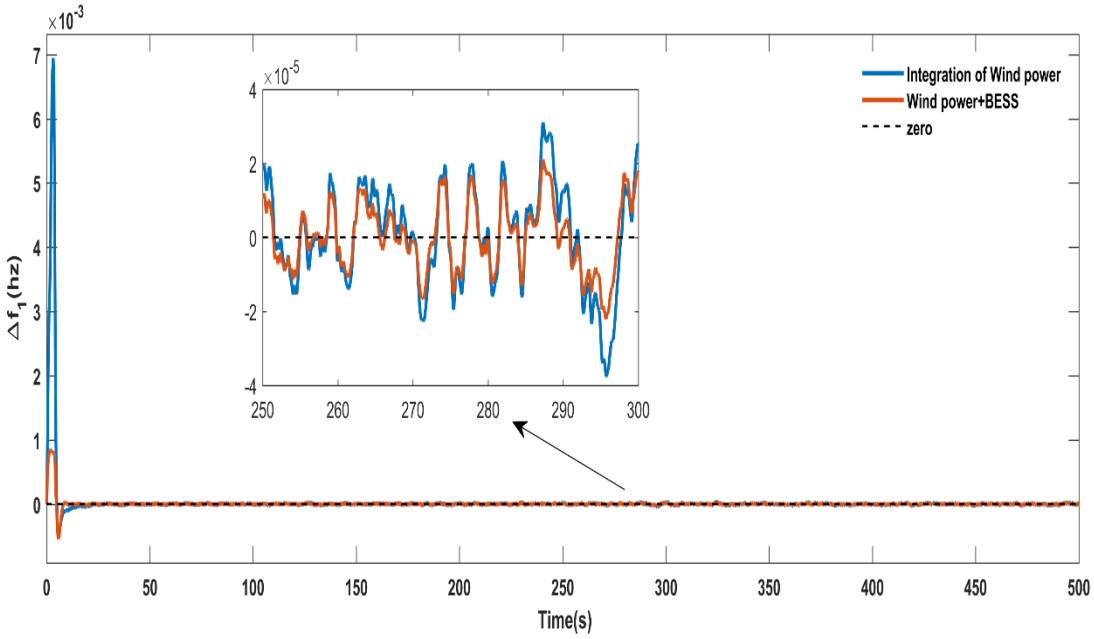

(a)

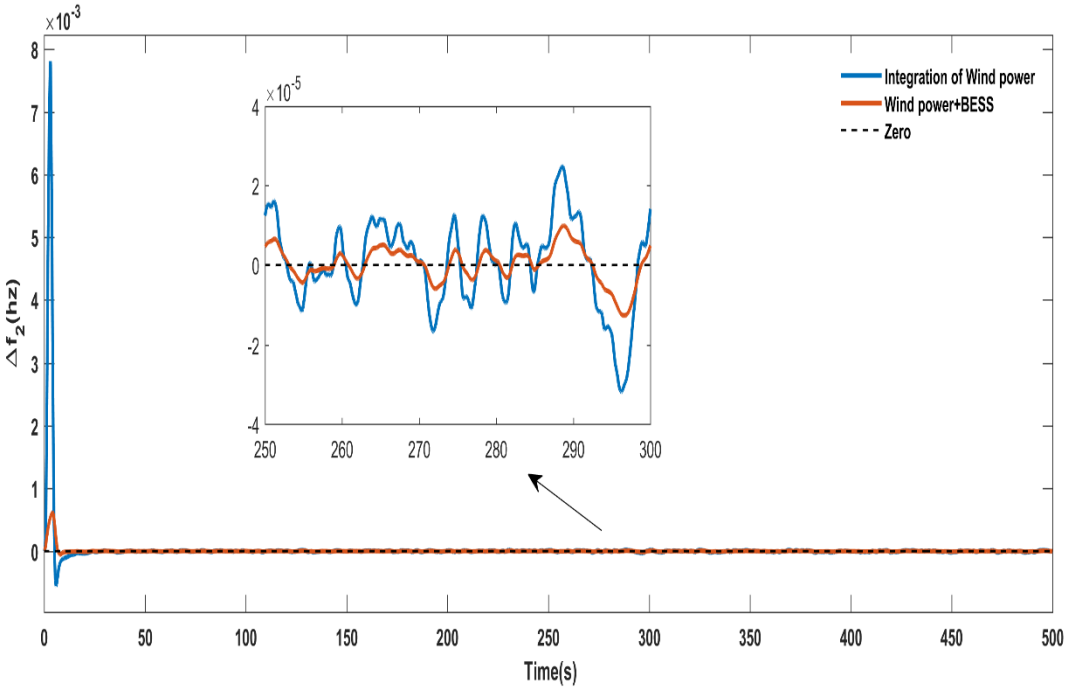

(b)

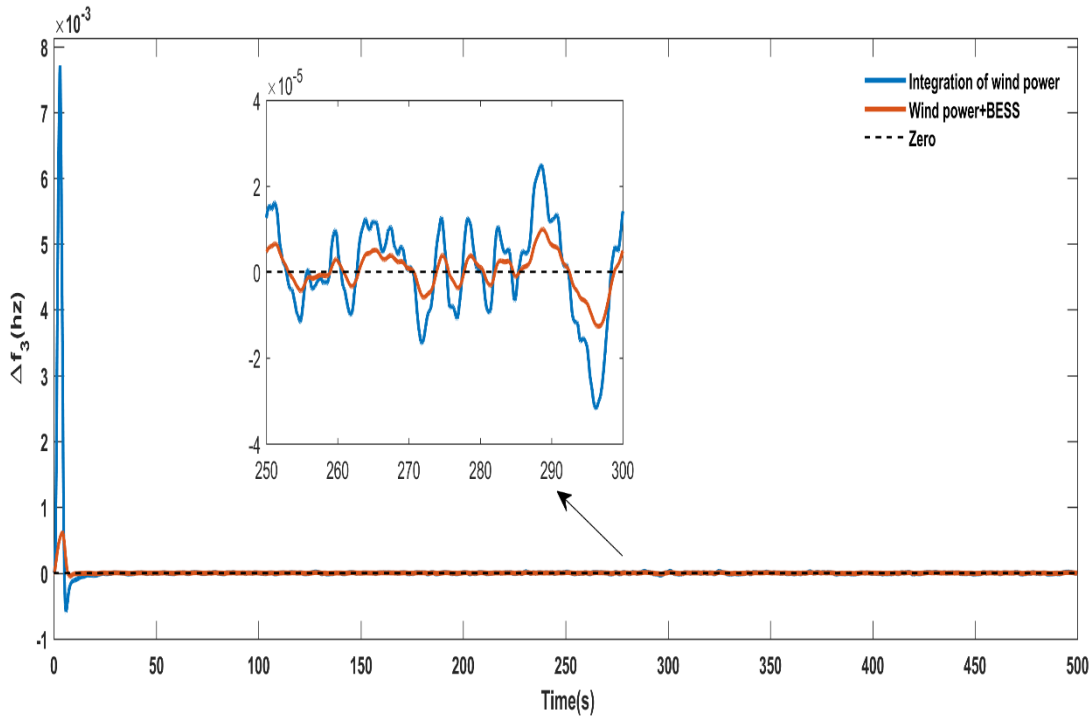

(c)

Figure 3.14: Dynamical response of (a): Δf_1, (b): Δf_2 and (c): Δf_3 with integration of wind power and BESS.

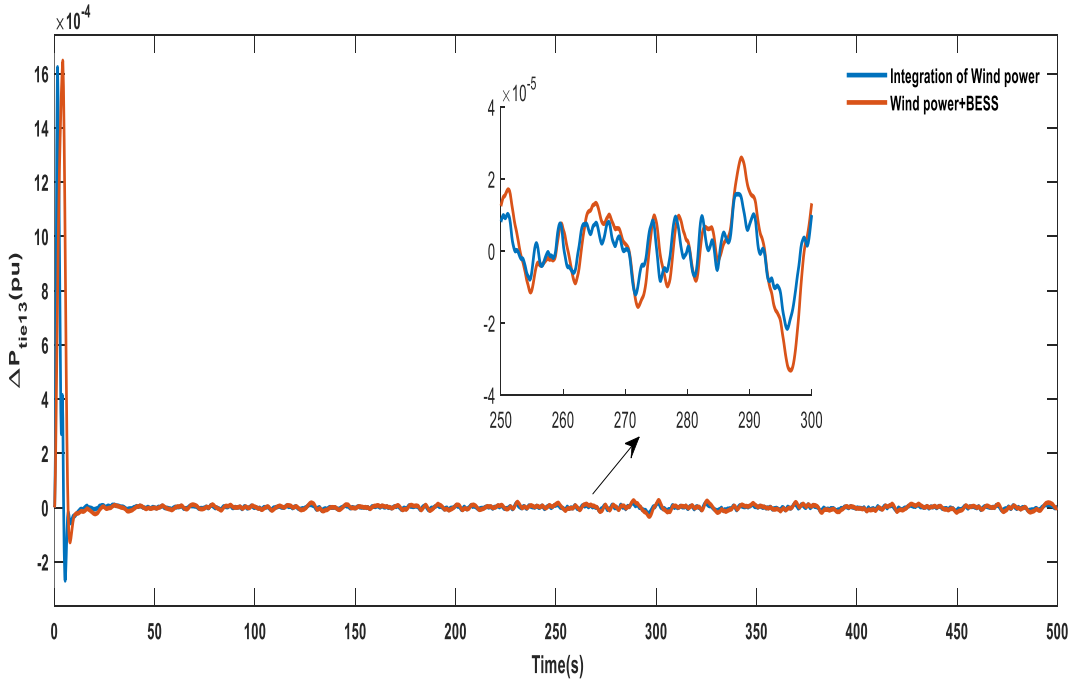

(a)

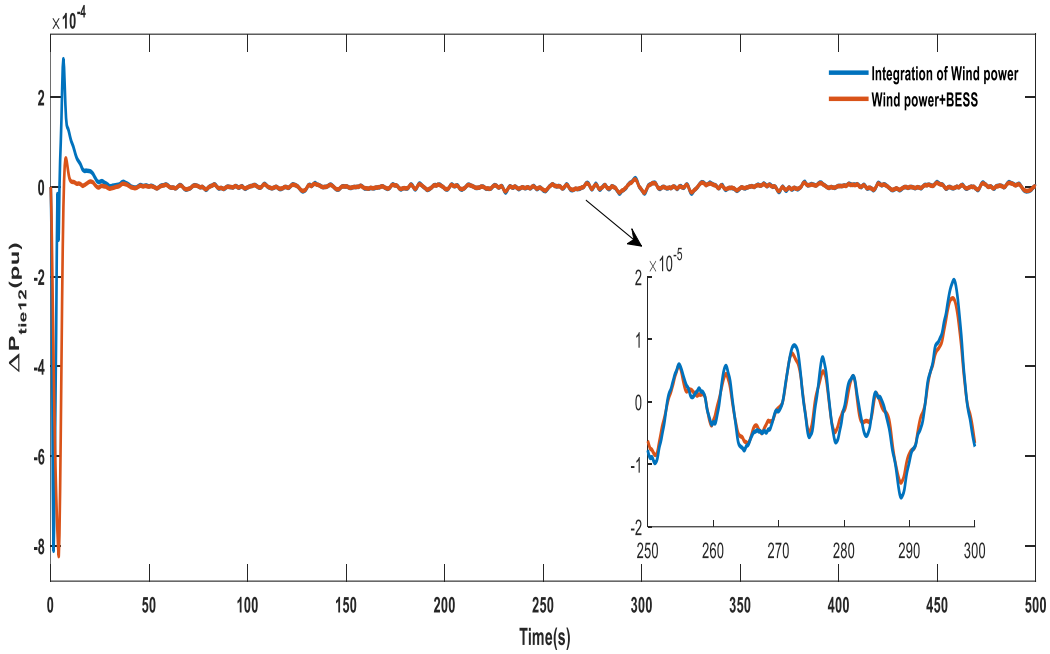

(b)

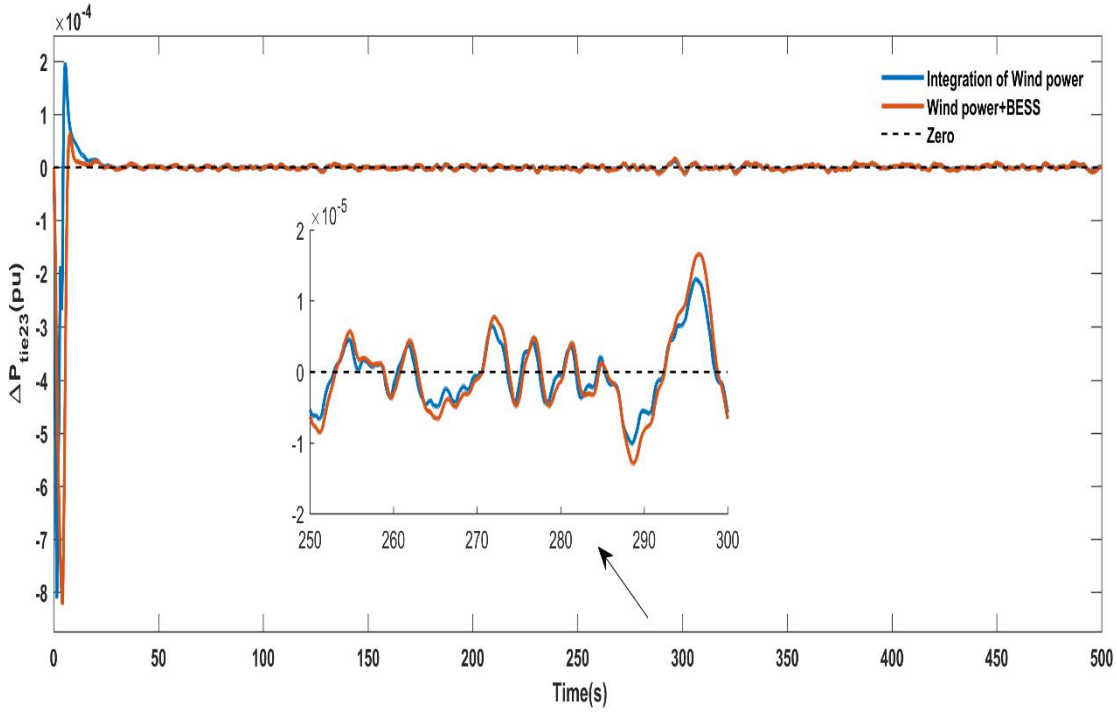

(c)

Figures 3.15: Dynamic response of (a): ΔP_{tie13}, (b): ΔP_{tie12} and (c): ΔP_{tie23} with integration of wind power and BESS.

From Figure 3.16 we can notice that in the presence of BESS, the value of ISE improves.

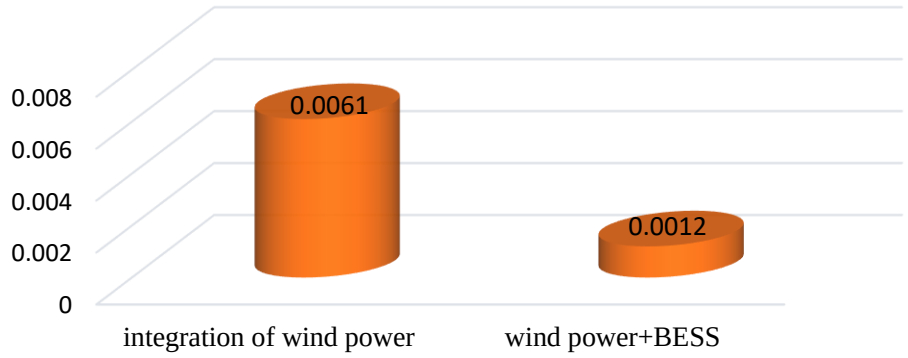

Figure 3.16: Comparison of ISE value of integration of Wind power and BESS

3.5 Conclusion

In this chapter, we looked at the investigations done in the three-area reheat system with acceptable GRC and GDB nonlinearities and wind power integration in area 1. Then executed the Archimedes optimization algorithm (AOA) on the system without the integration of wind power to obtain the optimum controller settings by Integral of the Squared Error (ISE) criteria; also, we compared this new algorithm (AOA) with another one which was the Genetic Algorithm (GA) to test its effectiveness. Then, we compared ISE values without BESS and with BESS. After that, we reached the system with BESS and without BESS. Finally, we compared the integration of wind power with and without a BESS battery.

General conclusion

General conclusion

In this work, the main goal of an electrical power system is to ensure the balance between the total power generation with the total load demand. For this purpose, we used classical controllers such as PID in the LFC problem's secondary control loop with wind power integration in the power system. We determined the optimal controller setting via a novel optimization algorithm known as the Archimedes optimization algorithm (AOA). In addition, we engaged Battery Energy Storage System (BESS) for better performance in restoring the system against various disruptions produced by wind power integration.

To achieve our goals, we are passed through several points as follows:

A non-linear LFC model of three interconnected zones under normal power system operation conditions was used to make the study more realistic. A reheat-thermal unit with the essential GRC, GDB composes each area. In the first study, investigations were carried out considering 1% Load Disturbance in the first area; we considered wind turbine load variation in the first area.

After that, we investigated the classical Proportional Integral Derivative (PID) for secondary controller design purposes. Next, the AOA has been used to define the optimal controller gains by Integral of the Squared Error (ISE) criteria with details. After that, we wanted to see how effective this new optimization method (AOA) was, so we compared it to another optimization algorithm, GA. From the results of the comparison that AOA is a better optimization than GA.

Then, we wanted to investigate how wind energy affected the electrical grid. As an observation, it was clear that the integration of wind power in power systems creates problems due to random wind speed.

Next, we got to clarify BESS's performance. As a result, we compared systems with and without BESS of ISE value under load disturbance. It was evident that the system with BESS surpassed the one without BESS.

At last, the suggested BESS can restore the system to a suitable state after various disturbances caused by wind power integration.

This memoir has discussed some essential points of control strategies in the LFC problem. For further research, the following suggestions are recommended:

- A suggestion of other control mechanisms for the LFC's design;
- Use of the storage system such as SMES in the LFC dynamics;
- Implement and test the Battery energy storage system on a real power system;

References

References

[1] S. c, C. Yammani, and S. Maheswarapu, ‘Load Frequency Control of Multi-microgrid System considering Renewable Energy Sources Using Grey Wolf Optimization’, *Smart Science*, vol. 7, no. 3, pp. 198–217, Jul. 2019, doi: 10.1080/23080477.2019.1630057.

[2] ‘The Electric Power Engineering Handbook - Five Volume Set’, *Routledge & CRC Press*. https://www.routledge.com/The-Electric-Power-Engineering-Handbook---Five-Volume-Set/Grigsby/p/book/9781439856352 (accessed May 22, 2022).

[3] H. Bevrani, ‘Decentralized Robust Load-frequency Control Synthesis in Restructured Power Systems’, p. 128.

[4] P. N. Topno and S. Chanana, ‘Tilt Integral Derivative control for two-area load frequency control problem’, in *2015 2nd International Conference on Recent Advances in Engineering & Computational Sciences (RAECS)*, Chandigarh, India, Dec. 2015, pp. 1–6. doi: 10.1109/RAECS.2015.7453361.

[5] A. Delassi, S. Arif, and L. Mokrani, ‘A novel Tilt Integral Derivative plus Second Derivative Order for Load Frequency Control problem in power system’, in *2016 8th International Conference on Modelling, Identification and Control (ICMIC)*, Algiers, Algeria, Nov. 2016, pp. 359–363. doi: 10.1109/ICMIC.2016.7804137.

[6] Delassi, Abdelmouméne. *Control Strategies for Automatic Generation Control in Interconnected Power Systems*. Diss. Université Amar Telidji de Laghouat, Département Electrique, 2016.

[7] M. R. I. Sheikh, R. Takahashi, and J. Tamura, ‘Multi-area frequency and tie-line power flow control by coordinated AGC with TCPS’, in *International Conference on Electrical & Computer Engineering (ICECE 2010)*, Dhaka, Bangladesh, Dec. 2010, pp. 275–278. doi: 10.1109/ICELCE.2010.5700681.

[8] H. Wang, H. Du, Q. Cui, and H. Song, ‘Artificial bee colony algorithm based PID controller for steel stripe deviation control system’, *Science Progress*, vol. 105, no. 1, p. 003685042210751, Jan. 2022, doi: 10.1177/00368504221075188.

[9] D. Ramey and J. Skooglund, ‘Detailed Hydrogovernor Representation for System Stability Studies’, *IEEE Trans. on Power Apparatus and Syst.*, vol. PAS-89, no. 1, pp. 106–112, Jan. 1970, doi: 10.1109/TPAS.1970.292676.

[10] H. Bevrani, *Robust Power System Frequency Control*. Cham: Springer International Publishing, 2014. doi: 10.1007/978-3-319-07278-4.

[11] S. W. Fardo and D. R. Patrick, *Electrical Power Systems Technology*, 3rd ed. River Publishers, 2020. doi: 10.1201/9781003151470.

[12] Kiam Heong Ang, G. Chong, and Yun Li, 'PID control system analysis, design, and technology', *IEEE Trans. Contr. Syst. Technol.*, vol. 13, no. 4, pp. 559–576, Jul. 2005, doi: 10.1109/TCST.2005.847331.

[13] R. Kansal and B. S. Surjan, 'Study of Load Frequency Control in an Interconnected System Using Conventional and Fuzzy Logic Controller', vol. 3, no. 5, p. 7, 2012.

[14] 'Power-System-Stability-and-Control-by-Prabha-Kundur (1).pdf'.

[15] R. K. Sahu, S. Panda, and U. K. Rout, 'DE optimized parallel 2-DOF PID controller for load frequency control of power system with governor dead-band nonlinearity', *International Journal of Electrical Power & Energy Systems*, vol. 49, pp. 19–33, Jul. 2013, doi: 10.1016/j.ijepes.2012.12.009.

[16] Saadat, Hadi, and Electrical Engineering Series. *Computational aids in control systems using MATLAB*. McGraw-Hill, 1993.

[17] N. N. Shah, 'The State Space Modeling of Single, Two and Three ALFC of Power System Using Integral Control and Optimal LQR Control Method', *IOSRJEN*, vol. 02, no. 03, pp. 501–510, Mar. 2012, doi: 10.9790/3021-0203501510.

[18] M. L. Kothari, P. S. Satsangi, and J. Nanda, 'Sampled-Data Automatic Generation Control of Interconnected Reheat Thermal Systems Considering Generation Rate Constraints', *IEEE Trans. on Power Apparatus and Syst.*, vol. PAS-100, no. 5, pp. 2334–2342, May 1981, doi: 10.1109/TPAS.1981.316753.

[19] J. Morsali, K. Zare, and M. Tarafdar Hagh, 'Appropriate generation rate constraint (GRC) modeling method for reheat thermal units to obtain optimal load frequency controller (LFC)', in *2014 5th Conference on Thermal Power Plants (CTPP)*, Tehran, Iran, Jun. 2014, pp. 29–34. doi: 10.1109/CTPP.2014.7040611.

[20] P. Bhatt, R. Roy, and S. P. Ghoshal, 'GA/particle swarm intelligence based optimization of two specific varieties of controller devices applied to two-area multi-units automatic generation control', *International Journal of Electrical Power & Energy Systems*, vol. 32, no. 4, pp. 299–310, May 2010, doi: 10.1016/j.ijepes.2009.09.004.

[21] Bavarva, Sagar R. "Green Chemistry Approaches to Renewable Energy." (2015).

[22] H. Bevrani, M. Watanabe, and Y. Mitani, *Power system monitoring and control*. Hoboken, New Jersey: Wiley, 2014.

[23] E. A. Mohamed and Y. Mitani, 'Load frequency control enhancement of islanded micro-grid considering high wind power penetration using superconducting magnetic energy storage and optimal controller', *Wind Engineering*, vol. 43, no. 6, pp. 609–624, Dec. 2019, doi: 10.1177/0309524X18824533.

[24] P. Aristidou, G. Valverde, and T. Van Cutsem, 'Contribution of Distribution Network Control to Voltage Stability: A Case Study', *IEEE Trans. Smart Grid*, vol. 8, no. 1, pp. 106–116, Jan. 2017, doi: 10.1109/TSG.2015.2474815.

[25] A. D. Hansen, 'Introduction to wind power models for frequency control studies', p. 31.

[26] T. Ackermann, Ed., *Wind power in power systems*, 2nd ed. Chichester, West Sussex ; Hoboken, N.J: Wiley, 2012.

[27] M. Milligan, B. Kirby, R. Gramlich, and M. Goggin, 'Impact of Electric Industry Structure on High Wind Penetration Potential', NREL/TP-550-46273, 962494, Jul. 2009. doi: 10.2172/962494.

[28] R. Rockafellar, "Fundamentals of Optimization," Dept. of Mathematics University of Washington 2007.

[29] P. N. Topno and S. Chanana, 'Tilt Integral Derivative control for two-area load frequency control problem', in *2015 2nd International Conference on Recent Advances in Engineering & Computational Sciences (RAECS)*, Chandigarh, India, Dec. 2015, pp. 1–6. doi: 10.1109/RAECS.2015.7453361.

[30] P. N. Topno and S. Chanana, 'Application of tilt integral derivative control on two-area power system', *J Engin Res*, vol. 4, no. 2, p. 12, Apr. 2016, doi: 10.7603/s40632-016-0012-4.

[31] X.-S. Yang, *Nature-inspired metaheuristic algorithms*, 2. ed. Frome: Luniver Press, 2010.

[32] F. A. Hashim, K. Hussain, E. H. Houssein, M. S. Mabrouk, and W. Al-Atabany, 'Archimedes optimization algorithm: a new metaheuristic algorithm for solving optimization problems', *Appl Intell*, vol. 51, no. 3, pp. 1531–1551, Mar. 2021, doi: 10.1007/s10489-020-01893-z.

[33] G. Haines, 'Basic Operation of a Battery Energy Storage System (BESS)', p. 14.

[34] E. Reihani, S. Sepasi, L. R. Roose, and M. Matsuura, ‘Energy management at the distribution grid using a Battery Energy Storage System (BESS)’, *International Journal of Electrical Power & Energy Systems*, vol. 77, pp. 337–344, May 2016, doi: 10.1016/j.ijepes.2015.11.035.

[35] S. c, C. Yammani, and S. Maheswarapu, ‘Load Frequency Control of Multi-microgrid System considering Renewable Energy Sources Using Grey Wolf Optimization’, *Smart Science*, vol. 7, no. 3, pp. 198–217, Jul. 2019, doi: 10.1080/23080477.2019.1630057.

Appendix

Appendix A

Three areas reheat thermal

Nominal parameters of the system investigated are:

B_1= B_2 =B_3 = 0,425 p.u. MW/Hz; R_1 =R_2 =R_3 = 2,4 Hz/p.u.; Tg_1 = Tg_2 = Tg_3 = 0,08 s; T_{T1} = T_{T2} = T_{T3} = 0.3 s; Kr_1=K_{r2}=K_{r3}=0.5s; T_{r1}=T_{r2}=T_{r3}=10s ;K_P = 120 Hz/p.u.; T_P = 20 s; T_{12} = 0,0866p.u. MW/rad; a_{12}=a_{13}=a_{23}=-1

Nonlinearities:

In this study, the GRC and GDB limits taken into account are given below: GRC = ± 10% per minutes = 0.0017 p.u. MW/min, GDB = ± 0.036 Hz.

Calculations with given Data of wind

Swept area $\boldsymbol{A} = 26^2 \times \pi$

Wind speed $\boldsymbol{v}$ = 8 m/sec

Air density $\boldsymbol{\rho}$ = 1.226 kg/m3

Power Coefficient $\boldsymbol{Cp}$ = 0.42

calculate the power converted from the wind

$P = \frac{1}{2}\rho A V^3 C_p$

$P = \frac{1}{2} \times 1.226 \times 26^2 \pi \times 8^3 \times 0.42$

Wind setting

T_{WT}=1.5

BESS settings

K_{BES}=-1.3

T_{BES}=0.1s

Appendix B

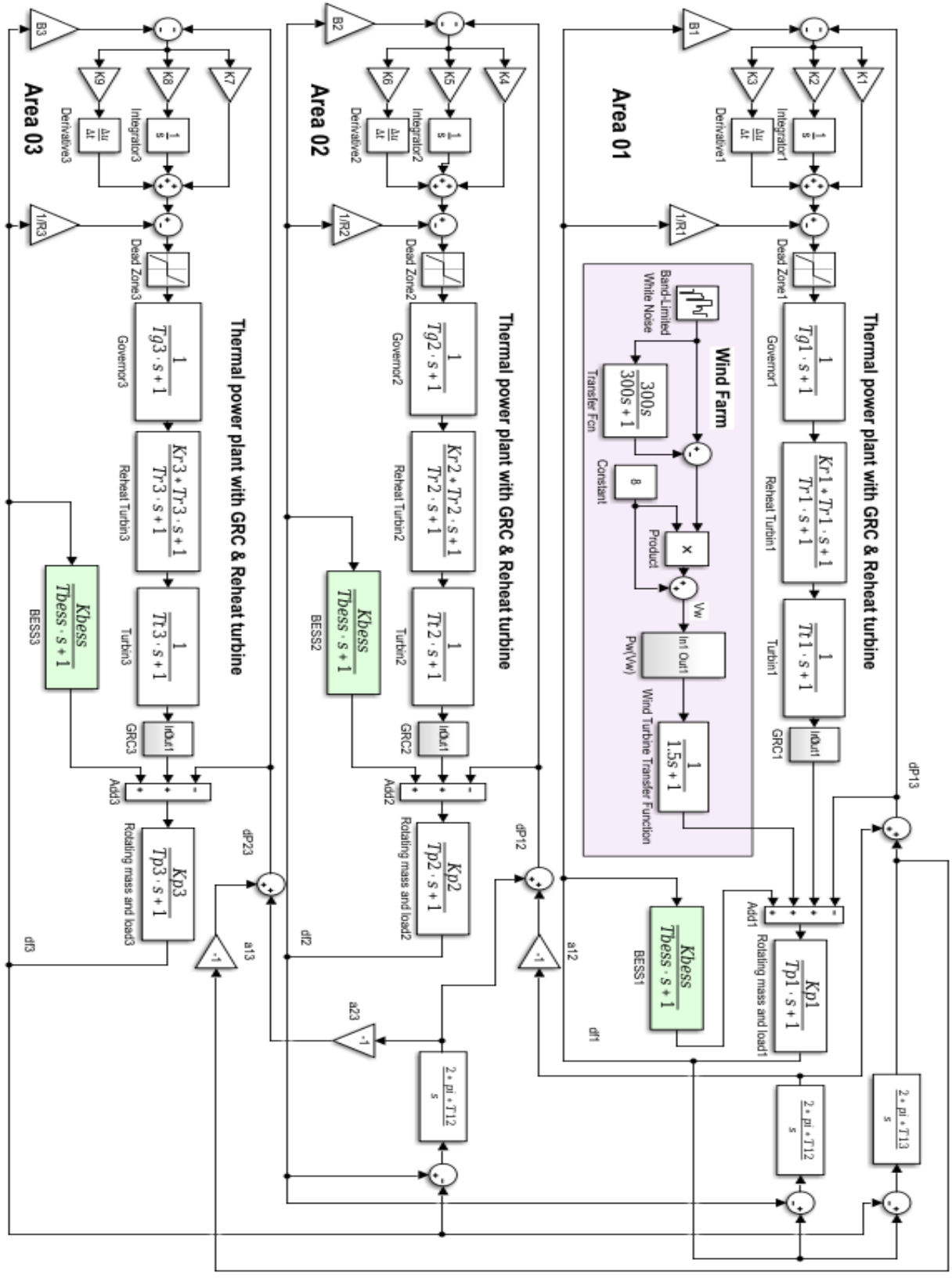
Area 01
Area 02
Area 03
Thermal power plant with GRC & Reheat turbine
Thermal power plant with GRC & Reheat turbine
Thermal power plant with GRC & Reheat turbine
Wind Farm
Band-Limited White Noise
Transfer Fcn
Constant
Product
Vw
Pw(Vw)
Wind Turbine Transfer Function
Dead Zone1
Governor1
Reheat Turbin1
Turbin1
GRC1
Add1
Rotating mass and load1
BESS1
Dead Zone2
Governor2
Reheat Turbin2
Turbin2
GRC2
Add2
Rotating mass and load2
BESS2
Dead Zone3
Governor3
Reheat Turbin3
Turbin3
GRC3
Add3
Rotating mass and load3
BESS3
Integrator1
Derivative1
Integrator2
Derivative2
Integrator3
Derivative3
dP13
dP12
dP23
a12
a13
a23
df1
df2
df3